UNIVERSITÀ DI PISA

DIPARTIMENTO DI FARMACIA

Corso di Laurea Specialistica in Chimica e Tecnologia Farmaceutiche

Tesi di laurea:

Synthesis of Fyn inhibitors as potential anticancer agents

Relatori: Prof. Filippo Minutolo
Dr.ssa Carlotta Granchi

Candidata: Jessica Caciolla **(Matricola n° 480337)**

Settore Scientifico Disciplinare: **CHIM-08**

ANNO ACCADEMICO 2015-2016

Contents

1. General Introduction

Fyn is a protein belonging to the Src family of nonreceptor tyrosine kinases (SFKs), which also includes Src, Yes, Lck, Lyn, Hck, Fgr and Blk.

It is a membrane protein localized in the inner layer of the cell membrane to which it is attached by binding with myristatic and palmitatic acids.

Fyn plays a key role in the regulation of many signaling pathways in both normal cells and in those cancer.[1] This protein is involved in various biological functions including growth factor and cytokine receptor signaling, cell-cell adhesion, platelet activation, T-cell and B-cell receptor signaling, ion channel function, integrin-mediated signaling, axon guidance, entry into mitosis and the differentiation of natural killer cells, oligodendrocytes, and keratinocytes.

The overexpression of Fyn leads to the stimulation of the proliferation and of cell growth, to the alterations of mitogenetic signals and morphogenetic changes; all these phenomena underlie the development of malignancies [2].

1.1. Gene and structure of kinase Fyn

Fyn is a 59 kDa protein which consists of 537 amino acids and encoded by the Fyn gene, located on chromosome 6q21. Nowadays, there are three know splice variants of Fyn that arise from alternative splicing of exon 7 of the Fyn gene [3].

Fyn has two types of exon 7, exon 7A and exon 7B, which produce the two major Fyn isoform : Fyn B (exon A) and Fyn T (exon B). These two forms differ in the sequence of about 50 amino acids that connect the end of the SH2 domain and the beginning of the SH1 domain. Fyn B and Fyn T have a different tissue distribution: Fyn T, the ancestral isoform, is expressed mainly in the hematopoietic system, while Fyn B is located in the central nervous system.

It is possible that this evolutionary divergence in the SH2- linker segment of Fyn T and Fyn B confers distinct regulatory features [4].

Then it has been described a novel isoform, Fyn Δ7, in which exon 7 is absent [5]. This form has been found in blood cells, but no translated protein has been documented.

Similarly to the majority of SFKs, Fyn is of a modular nature (**Fig. 1**); the domains of these proteins include a unique N-terminal sequence (SH4) , three protein modules including the SH3, SH2, and kinase domains (SH1) , and C-terminal tail [6].

Fig. 1: General linear protein structure of Fyn and the Src- family members. (Saito et all. 2010)

- The N-terminal SH4 domain is responsible for the interaction of kinases with cell membranes. The anchoring of the protein to the membrane is favoured by the specific acylation of two amino acids residues present in the consensus sequence Met- Gly- Cys of the N-terminal region. After removal Met, miristate is attached to the N-terminal Gly-2 via amide linkage, whereas the palmitoylation of Cys-3 occurs via a thioester linkage [7].
- The unique domain is different for each member of the family SFKs. The role of this sequence is still to be fully cleared but also likely to be required for the subcellular localization of the enzyme [8].

- The SH3 domain (~ 60amino acids residues) mediates intra- and inter-molecular protein- protein interactions necessary for the control of the enzymatic activity, for interaction with the substrates and for the subcellular localization. This domain is a β- barrel consisting of five antiparallel β- strands and two prominent loops called RT and n-Src loops. The interaction occurs via the recognition of polyproline motif (PxxP), present on the protein partner, that adopts a polyproline type II helical conformation that complexes with the SH3 domain.
- The SH2 domain (~100 amino acids residues), such as the SH3 domain, mediates intra- and inter- molecular protein- protein interactions. This domain consists of a central three- stranded β- sheet with a single helix packed against each side (α1 and α2). This domain forms two recognition pockets with which bind phosphotyrosine residues with a general pYEEI sequence : one binds the phosphorylated tyrosine and the other interacts with one or more hydrophobic residues C-terminal to the phosphotyrosine [9].
- The SH1 domain has the function to catalyse the transfer of a phosphate group from a molecule of ATP to a tyrosine residue of a substrate protein. This domain has a bilobal structure; the N- terminal (or small) lobe is composed by five β- strands and a single α-helix (also called C helix) which is an important component of the regulatory mechanism and the C-terminal (or large) lobe, containing the regulatory activation loop (A-loop), which is predominantly α-helical and it is the site of activating tyrosine phosphorylation.

  The large lobe contains the activation site where there is Tyr420 whose phosphorylation determines the complete enzyme activation.

  These two lobes form a pocket in which occur nucleotide binding (adenine moiety interacts with the N lobe and a short hinge segment that connects the two lobes) and phosphotransfer [10].

  The central core of the catalytic domain is a region with greatest frequency of highly conserved residues : DFG (Asp- Phe- Gly) and APE (Ala- Pro- Glu).

The aspartic acid residue may interact with the phosphate groups of ATP through Mg^{2+} salt bridges [11], this interaction is responsible for the correct positioning of the phosphate to be transferred from ATP to the protein substrate.

- The C- terminal region contains a critical tyrosine residue (Tyr531) involved in the regulation of protein activity. This residue is an inhibitory tyrosine that when phosphorylated binds to the SH2 domain to prevent the substrate binding [12].

1.2. Regulation of Fyn activation

The protein Fyn, as the other Src family kinases, has two regulatory tyrosine residue whose phosphorylation either activates (Tyr420) or inhibits (Tyr531) the activity of the kinase.

The equilibrium between tyrosine phosphorylation and dephosphorylation determines the intramolecular interaction that regulates the activity of Fyn.

The inactive conformation of the kinase is characterized by intramolecular interactions mediate by SH2 and SH3 domains. The SH2 domain binds the phosphorylated C-terminal tyrosine (Tyr531 residue of isoform Fyn [B] corresponding to the Tyr528 of the Fyn [T]) [13], while the SH3 domain binds the linker segment between the SH2 domain and the catalytic domain [14]. These structural modifications enable the SH2 domain to get closer to the large lobe and to the SH3 domain to approach the small lobe (**Fig.2**). The SH2 linker segment seems to serve as an adapter for the interaction of the SH3 and of catalytic domain. These assumed positions determine the distortions of the catalytic site such as to render it inactive [15]. In particular, the hydrogen bond between Glu in the αC- helix and Lys, required for Mg-ATP binding, is disrupted in the inactive conformation. The dephosphorylation of Tyr 531 causes conformational change in the kinase domain that leads to the formation of a hydrogen bond between Glu and Lys in the catalytic

domain. The enzyme is now in active form and can catalyze the intramolecular auto-phosphorylation of Tyr420 in the activation loop. Thus the catalytic domain is in the active conformation allowing the access of substrates to the active site.

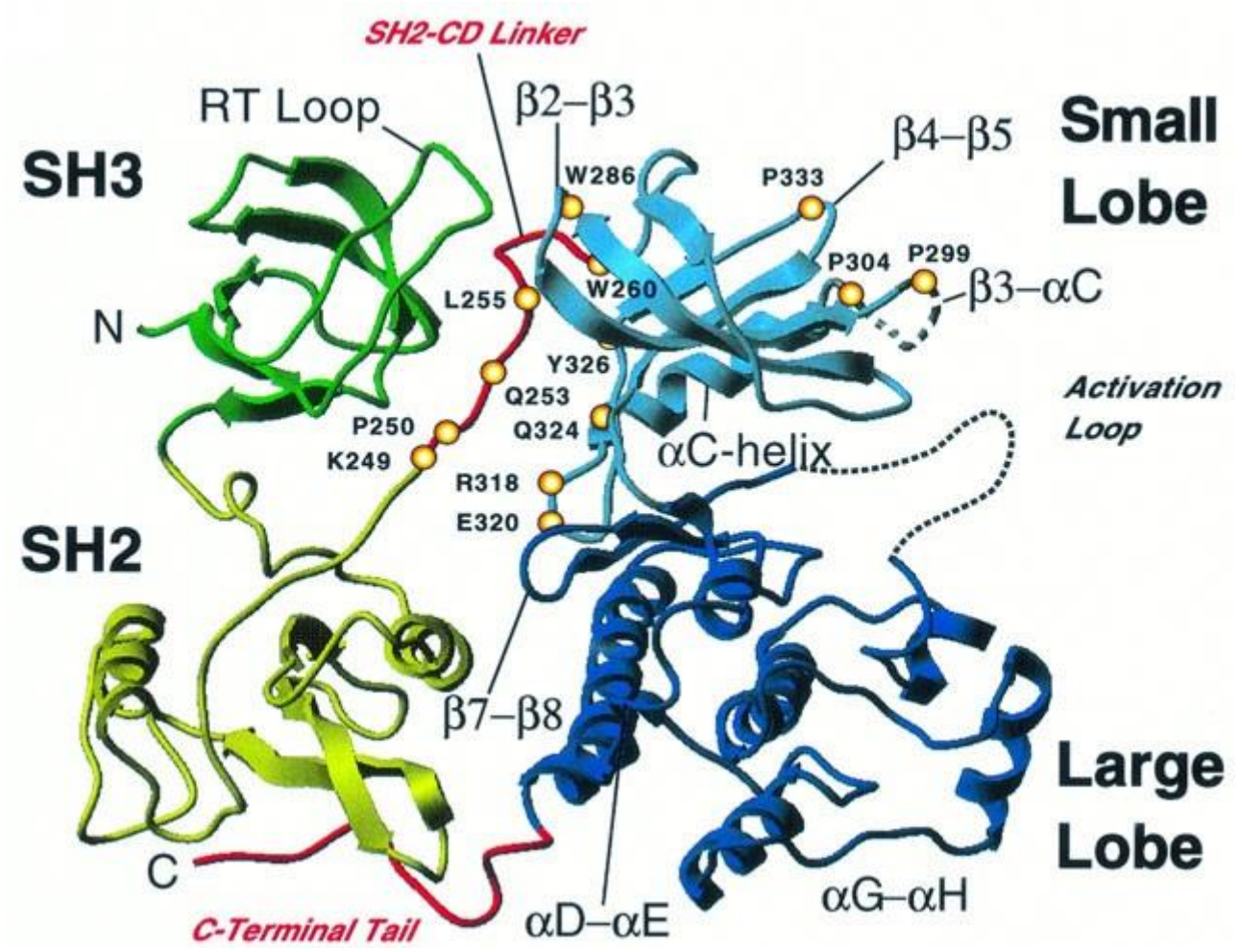

Fig. 2: Structure of Src family kinases

SFKs can also be regulated by interaction with molecules that compete with the SFKs domains. Interactions with these proteins destroy the inactive stabilized conformations of SFKs and promote the phosphorylation of these proteins by SFKs. Overall, full activation of SFKs seems to proceed in the following order:

- The substrate binds the SH2/3 domains of inactive SFKs to destabilize, and thus open, the closed conformation;
- Tyrosine phosphatase dephosphorylate the Tyr531 to stabilize the active conformation;
- Finally, SFKs undergo intermolecular auto-phosphorylation on Tyr 420. In this way, the catalytic pocket is locked into the active conformation [16].

Some enzymes responsible for inactivation of the kinase are: Csk (C-terminal Src kinase), which phosphorylates Tyr531 residue and STEP61 (striatal enriched phosphatase 61) which dephosphorylates Tyr420 residue[17]. In contrast, RPTPα (receptor protein tyrosine phosphatase-α) can activate the protein Fyn dephosphorylating Tyr531 residue[18].

1.3. Fyn and central nervous system function

Fyn performs important functions in the development and regulation of numerous functions of the central nervous system (CNS). This protein is found in many areas of the brain, including glial cells, in white matter tracts and in cultured oligodendrocytes. Fyn has been shown to be important for CSN myelination (formation of a myelin sheath around nerve fibers) and it appears to promote the morphological differentiation of oligodendrocytes. Evidence shows that Fyn tyrosine kinase is activated during the initial stages of myelination and that it couples to MAG (large myelin-associated glycoprotein), F3 and NCAM120 (120kDa neural cell adhesion molecule). Fyn mutant mice have a deficit of myelin content in the forebrain [19].

It has been demonstrated that in oligodendrocytes Fyn interacts with α-tubulin , a member of the tubulin family involved in the nucleation and in the polar orientation of microtubules, cytoskeletal structures essential for the formation of neurites. In addition, Fyn binds cytoskeletal protein Tau, and this interaction facilitates the

outgrowth of oligodendrocytes processes. Tau interacts with the Fyn SH3domain whereas α-tubulin binds to the SH2 and SH3 domains [20].

The lack of a functional Tau-Fyn interaction may underlie of some human CSN degenerative diseases such as multiple sclerosis where axonal degeneration is a defining aspect of the clinical decline [21].

Fyn is localized to the post-synaptic density (PSD), a receptor complex consisting of several receptors such as PSD95 (postsynaptic density protein 95), NMDAR (N-methyl-D-aspartate receptor), and AMPAR (α-amino-3-hydroxy-5-methyl-4-isoxazolepropionic acid receptor). These neurotransmitter receptors and signalin proteins trigger neuronal excitation of the postsynaptic cells[22]. The NMDARs form a complex with PSD-95 through interactions between the cytoplasmic C-terminal tails of their NR2 subunits and the PDZ domains of PSD-95; in this way NMDARs are anchored in the PSD[23]. Fyn regulates the phosphorylation and trafficking of NMDA through interactions with glutamate receptor subunits NR2A and NR2B, so Fyn induces a potentiation of synaptic NMDA- mediated [24]. Fyn is also important for the regulation of the formation of dendritic spines, protrusions which represent the single contact points between an axon and a dendrite critical for synaptic function and plasticity. Fyn knockout mice show an age-dependent loss of dendritic spines.

For these reasons, Fyn seems to be involved in neurodegenerative disorders such as Alzheimer's disease (AD) [25].

1.4. Fyn kinase in Alzheimer's disease and other tauopathies

Alzheimer's disease is a chronic neurodegenerative disorder characterized by the presence of amyloid-β plaques and (Aβ) and neurofibrillary tangles. The mechanisms that define the disease are still unclear but it appears that a deregulation of Fyn protein is involved in AD pathogenesis. It was already mentioned in the previous

paragraph, Fyn is involved in synaptic plasticity. In addition, Fyn regulates Aβ production, mediates Aβ-induced synaptic deficits and neurotoxicity, and induces tyrosine phosphorylation of Tau [26].

The first step, that triggers Alzheimer's disease, seems to be the interaction between soluble oligomers of amyloid-β (Aβo) and cellular prion protein (PrP^c). This bond is specific for oligomeric form, with little or no affinity for fibrillary or monomeric Aβ peptide. Once the Aβo- PrP^c connection is formed, transformations at the level of neuronal biochemistry occur (**Fig.3**) and Fyn is activated by phosphorylation the Tyr 420 residue.

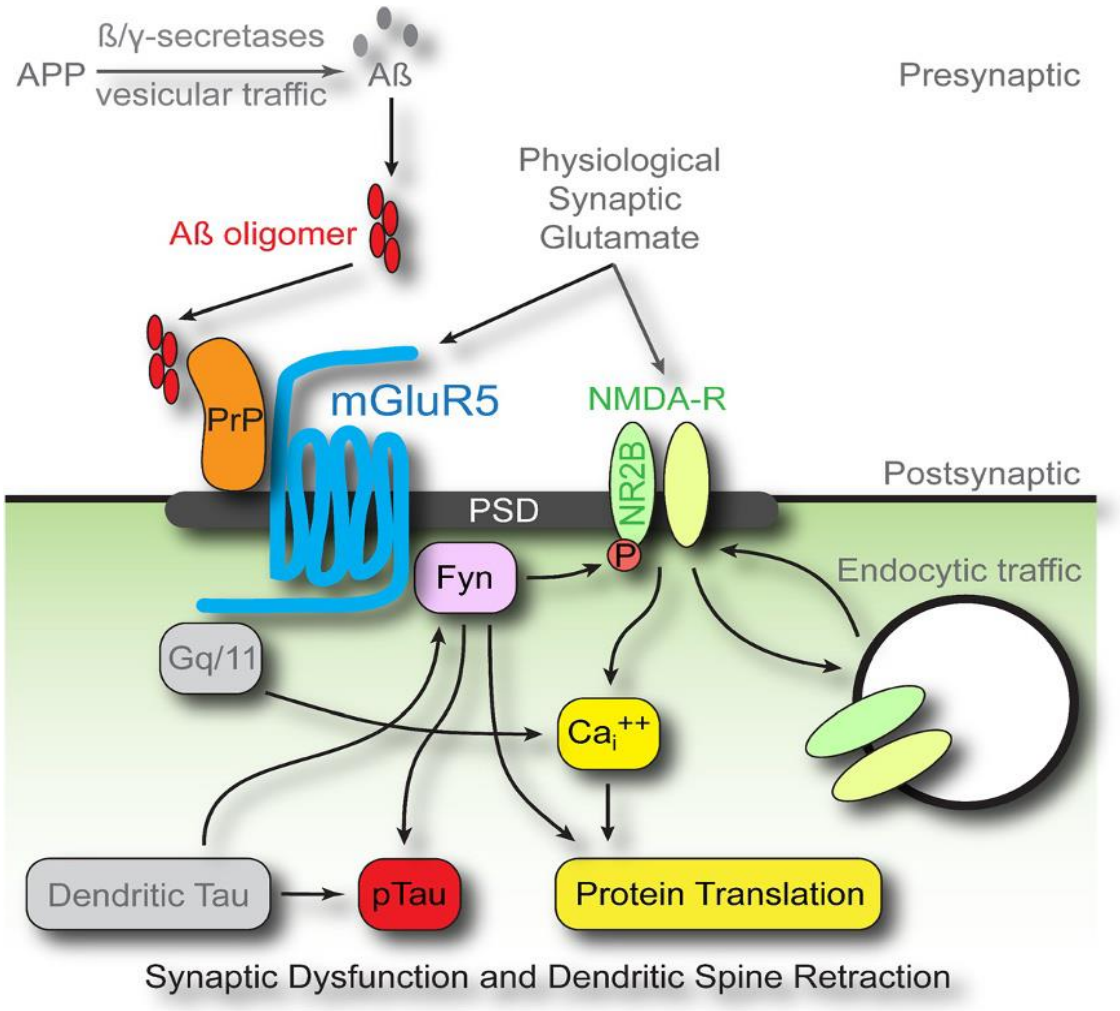

Fig. 3: mGluR5 couples amyloid-beta oligomer–cellular prion protein to post-synaptic signaling. Schematic illustrating a central role of Fyn in amyloid-beta oligomer (Aβo) signaling. Binding of Aβo to cellular prion protein (PrPC) triggers mGluR5-dependent signaling events. Proteins are clustered in the post-synaptic

density (PSD) and alter N-methyl-D-aspartate receptor (NMDA-R) function, calcium and protein translation. Tau plays a role in localizing Fyn and is a Fyn substrate. The net result of aberrant PrPC–mGluR5–Fyn signaling is synaptic malfunction and loss. Aβ, amyloid-beta; APP, amyloid precursor protein; PrP, prion protein.(Nygaard et all. *Alzheimer's Research & Therapy*, 2014)

To have the interaction between the complex Aβo- PrP^c and the Fyn protein is required the presence of metabotropic glutamate receptor (mGluR5), a transmembrane protein that links the extracellular levels of glutamate to calcium mobilization, to protein translation in dendrites and to tyrosine kinase signaling.

Fyn, after being activated, performs various functions including the phosphorylation of NR2A and NR2B subunits of the NMDA receptor. Several in vitro studies have shown dendritic spine loss after an acute Aβo exposure. This destabilization of dendritic spines due to Aβo is not observed in $Fyn^{-/-}$ cultures, this shows that Fyn plays a key role in Aβ-induced sinaptotoxicity .

In addition, Fyn is also involved in Tau phosphorylation. It is well known that, in addition to Aβ plaques, another distinctive feature of Alzheimer's disease is the presence of deposits of neurofibrillary tangles containing the hiperphosphorylated Tau protein[27]. Of the five tyrosine residues present in the protein Tau, only Tyr 18 is phosphorylated by Fyn. This residue, in fact, is located in the amino acid sequence GTYG which shows high homology with the canonical substrate sequence determined for Fyn (ETYG). Tau interacts with the SH3 domain of Fyn through a PXXP motif (pro233- pro236) [28].

In Alzheimer's disease it has been observed a possible interaction and synergistic effects between Tau protein and amyloid-β. Tau has a function to target Fyn to the dendritic compartment, in this way Fyn phosphorylates NMDA receptors and mediates the interaction with PSD95, an interaction required for amyloid-β toxicity [29].

Fyn is also able to phosphorylate α-sinuclein, a presynaptic protein implicated in various neurodegenerative diseases such as Alzheimer's and Parkinson's. Mutation

analysis revealed that the phosphorylation takes place specifically on Tyr125 [30]; this phosphorylation is blocked by the inhibitor PP2.

1.5. Fyn in cancer

As previously reported, the protein Fyn is involved in numerous cellular functions including growth and cell proliferation, morphogenesis and cell motility; anomaly affecting these processes are the basis of the development of tumours. It has been observed that an overexpression of Fyn determines the morphological changes in normal cells that support the development and progression of cancer [3].

It has been shown that Fyn is an important protein in the PIKE-A/ AMPK pathway.

In addition to the well-characterized functions as a regulator of the metabolic balance, AMPK is also involved in cell proliferation, cell growth, cell survival and autophagy.

PIKE-A interacts directly with AMPK and blocks its tumour suppressive function; this interaction is mediated by tyrosine kinase Fyn. Fyn phosphorylates PIKE-A on Tyr682 and Tyr774, increasing, in this way, the binding affinity by PIKE-A for AMPK [31].

In addition, this phosphorylation mediated by Fyn protein has a further antiapoptotic effect, going to inhibit the apoptotic degradation of PIKE-A . Point mutation of aspartate into alanine has highlighted that D474 and D592 are the main points of apoptotic degradation. The fact that Y682F and Y774F mutants enhance the apoptotic cleavage, while the degradation is relieved in vivo after stimulating with EGF, suggests that the phosphorylation of PIKE-A prevents its caspases induced cleavage under apoptotic condition and promotes cell survival. Fyn and PIKE-A form a complex through the bind between the Arf- GAP domain on PIKE-A and the SH1 domain of Fyn [32,33].

The PI3K/Akt/PKB is often implicated in the growth of the cancer cell and it has been demonstrated that Fyn and other SFKs play an important role in the regulation of Akt activity, through phosphorylation of tyrosine residues. In several cell lines it

was observed that EGF- induced tyrosine phosphorylation and kinase activity of Akt are both blocked by PP2, a Src family tyrosine kinase inhibitor. Then, two tyrosine residues were identified, Tyr 315 and Tyr 326, which are phosphorylated by Fyn and other SFKs, and whose replacement with two residues of phenylalanine causes a decrease in the kinase activity of Akt in response to growth factors.

These data suggest that Src family kinases directly regulate Akt activity[34].

SFKs also seem to be involved in cell migration, the process at the base of metastatic disease. Metastasis are determined by the ability of cells to migrate and interact with its local microenvironment. Important molecules involved in the control of cell adhesion and cell migration are the integrins, cell surface receptors that link extracellular matrix (ECM) with cytoskeletal proteins. FAK (focal adhesion kinase) is a tyrosine kinase which transmits the adhesion signal coming from integrins to the intracellular signalling cascade . FAK binds the β-subunit of integrin inducing, in this way, its autophosphorylation at Tyr597 and creating a binding site for SFKs. This complex (SFK- FAK) is further activated by phosphorylation at other sites, maximizing tyrosine kinase activity of FAK [35].

In addition, the Fyn protein interacts with PXL (paxillin), an important regulator of cell shape. It was observed that the overexpression of Fyn in human pancreatic cancer is accompanied by an up-regulation of FAK and PXL, two elements crucial to motility, and thus to invasion. These are cellular processes necessary for metastatic competence and the acquisition of the metastatic phenotype [36].

Another pathway through Fyn regulates cell shape and motility is its interaction with the Rho family of GTPases. Rho family GTPases is a subfamily of the Ras superfamily that is involved in regulating the intracellular actin dynamics and it includes Rac1, RhoA and Cdc42 [3]. In fibroblast, Cdc42 and Rac1 activation is associated with lamellipodia and filopodia, respectively, whereas activation of RhoA induces stress fiber formation. It is likely that Rac, RhoA and Cdc42 are involved in the control of morphological differentiation of some cells such as oligodendrocytes [37].

In addition to activating FAK, some integrins like α5β1, α1β1, α6β4, and $\alpha_v\beta3$, are able to interact and activate the Src- family kinase Fyn, that in turn activates the adaptor protein Shc. For this interaction, caveoli-1 works as a membrane adaptor that facilities the coupling of the α subunit of integrin to the Fyn protein. Fyn then phosphorylates Shc at Tyr317, forming an activated complex that combines with GRB2-SOS, causing activation of the Ras- ERK cascade [38]. Ras stimulates a kinase cascade that culminates in the activation of the mitogen- activated protein kinase (MAPK) ERK. The activation of this pathway results in the progression through the G1 step of the cell cycle in response to mitogens.

The integrin/ SFK-Shc/ Ras- ERK pathway (**Fig. 4**) connects cell adhesion with the progression of the cell cycle in a process called anchorage- dependent cell growth. Normal cells need to adhere to serum-derived extracellular matrix components for cell growth in vitro, on the contrary, the growth of tumour cells occurs also without adhering to the extracellular matrix. The overexpression of Fyn found in cancer cells can, thus, lead to deregulation of anchorage- dependent cell growth [39].

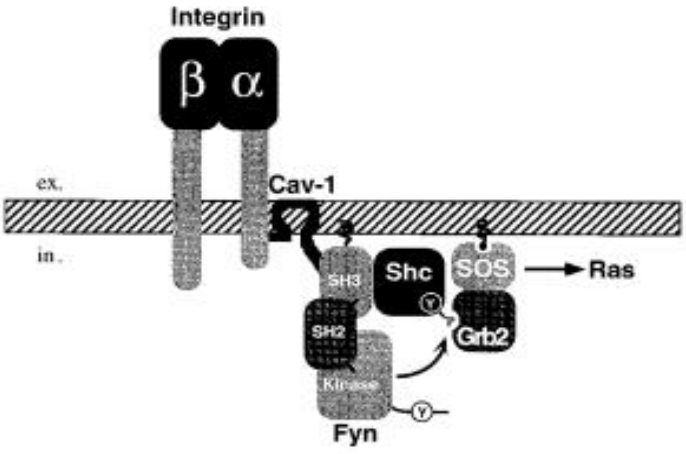

Fig. 4: Model of integrin- mediated recruitment of Shc and activation of Ras (Wary et all. *Cell*, 1998)

Fyn has been shown to be involved in the regulation of the rigidity of extracellular matrix surface. The matrix rigidity is important both for cell motility and that pathological events such as tumour formation and metastasis. One of the molecules involved in matrix force transduction is receptor- like protein tyrosine phosphatase-α (RPTP-α). RPTP-α forms a complex with $\alpha_v\beta_3$ integrin and actives Fyn by dephosphorylation of a negative regulatory phosphotyrosine presents in C-terminal domain. The palmitoylation site is very important for the activation of Fyn. As the Fyn is both myristoylated and palmitoylated, it has a high affinity for the cell membrane, on the contrary, the other Src, being only myristoylated, have a low affinity for the membrane and are not recruited by RPTP-α .

In addition, the level of Fyn activation is thought to be force- dependent in which greater forces result in greater reinforcement of integrin- cytoskeleton linkages.

Cas, the main substrate that is phosphorylated by Fyn, is required for the rigidity response and is localized to the leading edge in close proximity to Fyn [40].

It seems that cancer cells spread aggressively because the overexpression of Fyn leads to an exaggerated response to the rigidity of the extracellular matrix .

Fyn facilities the formation of metastases and cell migration, promoting the Epithelial-mesenchymal transition (EMT). EMT is a process characterized by loss of cell adhesion, a switch from E-cadherin to N-cadherin and an increase in cell motility, in which there is a transformation of the epithelial cell phenotype in a mesenchymal phenotype.

It has been observed that β6- integrin is expressed during the mesenchymal transition conferring the motile phenotype on SCC (squamous cell carcinoma) cells. β6-integrin interacts and actives Fyn, this coupling is required for the progression through EMT.

The presence of E-cadherin is the characterizing element of the epithelial phenotype and there is a direct link between the downregulation of E- cadherin with the increase of N-cadherin. Furthermore it seems to be a direct link between N-cadherin and Fyn activation [41].

The formation of the complex β6-integrin-Fyn seems to upregulate the expression of the MMP-3 (matrix metalloproteinase 3) gene. This event promotes oral SCC cell proliferation and metastasis in vivo [42].

These findings suggest that Fyn has a role as mediator of metastatic disease and of local tumour growth.

1.6. Fyn kinase inhibitors

Being involved in numerous pathway that underlie the development of various diseases, the protein Fyn became a very interesting pharmaceutical target for neurodegenerative pathologies and tumours.

Although the Fyn can theoretically be inhibited by molecules able to interact with some of the various domains present in its structure, most of the inhibitors present in the literature bind to the enzyme's catalytic site, by competing with the endogenous substrate (ATP).

Among the data available in the literature, only one X-ray structure of Fyn complexed with an inhibitor (staurosporine) has so far reported (2DQ7 PDB code).

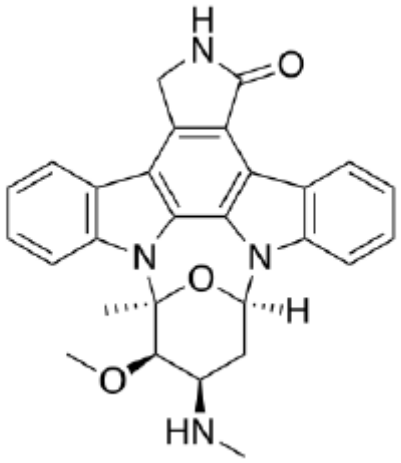

Fig. 5: Structure of staurosporine.

Staurosporine is a no selective inhibitor (**Fig. 5**) that binds to the ATP binding site, by three hydrogen bonds, a CH-O interaction, and some hydrophobic interactions (**Fig. 6**). The binding site is located in the pocket placed between the N- and C- lobes of the SH1 domain. The NH and keto oxygen of the amide function of the lactam ring of the staurosporine form two hydrogen bonds, respectivally, with the backbone carbonyl oxygen of Glu 342 and the backbone NH of Met344. These residues define the "hinge region" that is responsible for binding of the adenine ring of ATP to the catalytic site. Finally, the methylamino nitrogen of the glycosidic ring formed a hydrogen bond with Ser348. Staurosporine has a nanomolar inhibitory activity against Fyn (IC_{50} of 4.8 nM) [6].

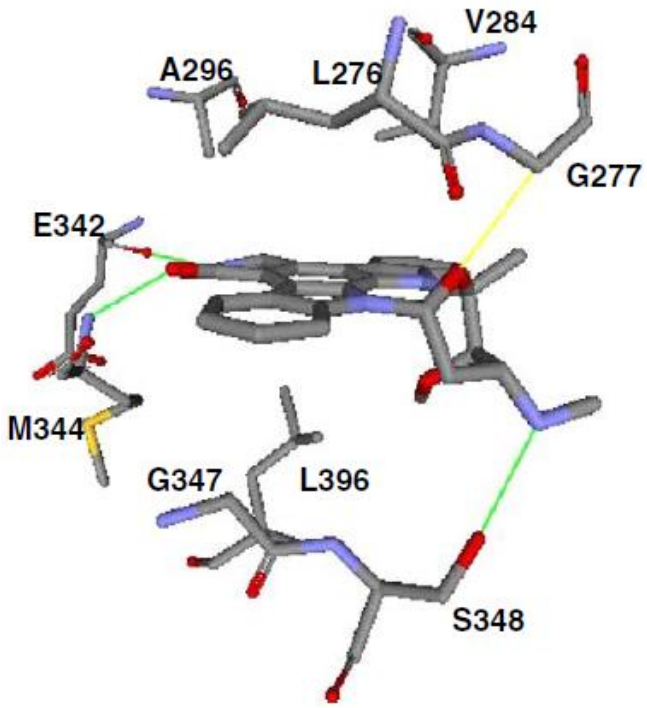

Fig. 6: Stereo-diagram of the significant residues for staurosporine binding. Three hydrogen bonds and a CH–O interaction are shown by green and yellow lines, respectively (Kinoshita et all. *Biochemical and Biophysical Research Communications*, 2006).

Agents targeted specifically against Fyn have not been developed clinically yet. Among tyrosine kinase inhibitors, some also show an inhibitory activity against Fyn.

1.6.1. PP1and PP2

These two compounds, belonging to the class of pyrazolo [3,4-d] pyrimidine (**Fig. 7**), were the first inhibitors to show a combination of power and selectivity for members of the Src family. They are ATP-competitive inhibitors that bind to the catalytic site of kinase, where the pyrazole- pyrimidine system takes the place the ATP adenine.

PP1 and PP2 have a nanomolar inhibitory activity with IC_{50} of 6 and 5 nM, respectively [43].

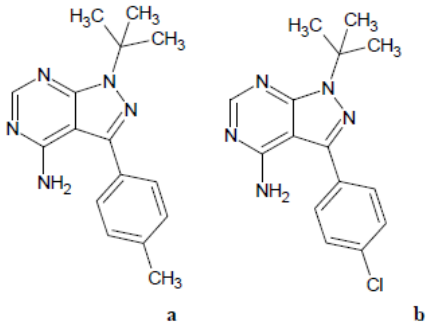

Fig. 7: Structures of compounds PP1 (**a**) and PP2 (**b**).

1.6.2. Compound 6f

This molecule (**Fig. 8**) belongs to a series of PP1 and PP2 analogues and it shows a good inhibitory activity against Fyn, with an IC_{50} of 40 nM (whereas in the same conditions in which the assay were made, the IC_{50} of PP1 is of 50 nM) [44].

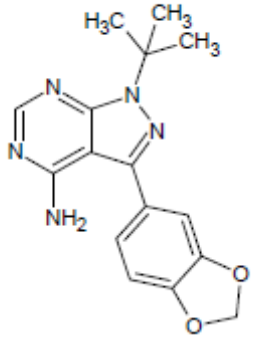

Fig. 8: Structure of compound 6f.

1.6.3. AP23546

This derived purine (**Fig. 9**) shows excellent potency for inhibition of Src family kinase with an IC_{50} against protein Fyn of 0.2 nM. This inhibitor exhibits *in vivo* toxicity that renders it unsuitable, however, its potency and selectivity make it ideal to examine tumorigenic functions mediated by SFKs [45].

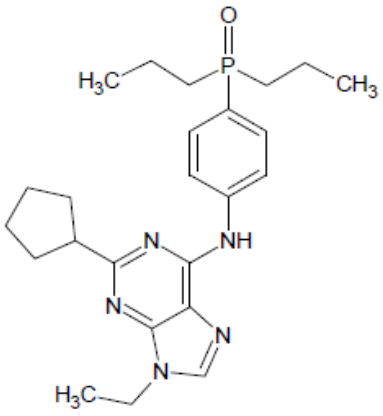

Fig. 9: Structure of AP23846.

1.6.4. BMS-279700

This compound, synthesized by Chen et all., is an anilinoimidazo[1,5-*a*]pyrido[3,2-*e*]pyrazine analogue (**Fig. 10**), which has shown to be active against SFKs. BMS-279700 has a nanomolar inhibitory activity against Lck, Src, Lyn and Fyn, with an IC_{50} towards the latter of 5 nM [46].

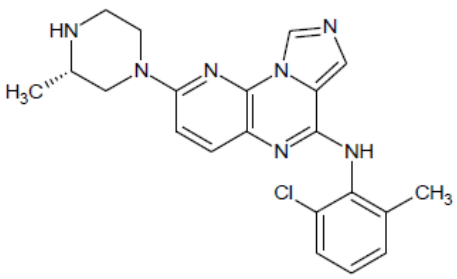

Fig. 10: Structure of BMS-279700.

1.6.5. CT5102, CT5263, CT5264, CT5269 and CT5276

These molecules (**Fig.11**), belonging to a novel series of Src kinase inhibitors, are more potent and selective for Src kinase enzymes than previous inhibitor, such as PP1. The five compounds examined exhibit excellent inhibitory activity against Fyn, with an IC_{50} ranging from 8 nM (CT5102) to 24 nM (CT5264) [47].

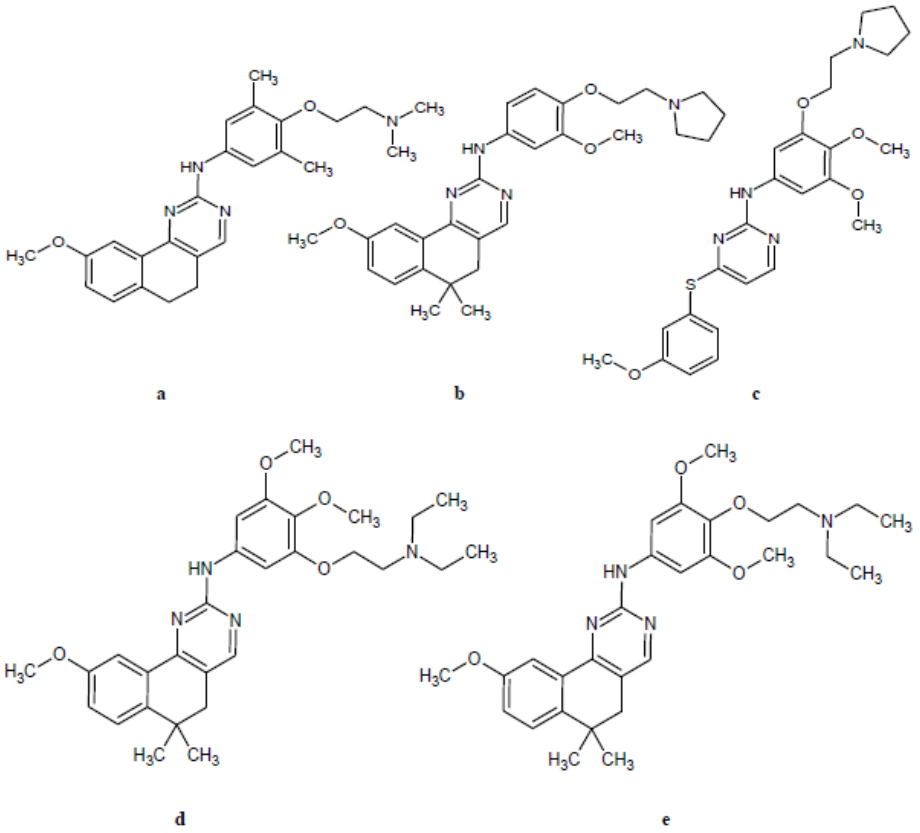

Fig. 11: Structure of compounds CT5102 (**a**), CT5263 (**b**), CT5264 (**c**), CT5269 (**d**) and CT5273 (**e**).

1.6.6. AZD0530

This compound, known as **sarcatinib** (**Fig. 12**), is an orally available SFKs inhibitor. AZC0530 has demonstrated potent antimigratory and antiinvasive effects *in vitro* and it presents a good inhibitory activity against Fyn, with an IC_{50} of 10 nM [48].

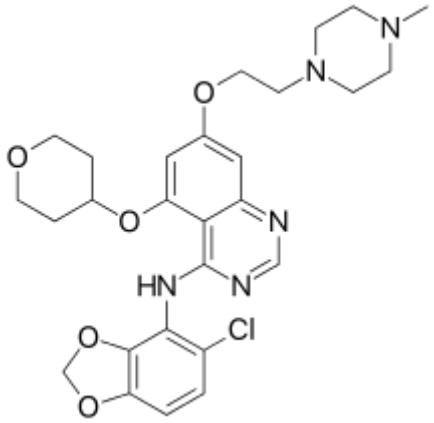

Fig. 12: Structure of sarcatinib.

1.6.7. BMS-354825

This molecule, known as **dasatinib** (**Fig. 13**), is an exquisitely potent inhibitor of the Src family kinases. It is a highly potent ATP competitive inhibitor and the lack of selectivity of this compound among Src family kinases is not unexpected, because the kinase domain is known to be highly conserved. It has subnanomolar IC_{50} against many kinases, as the case of Fyn (IC_{50} 0.2 nM) [49].

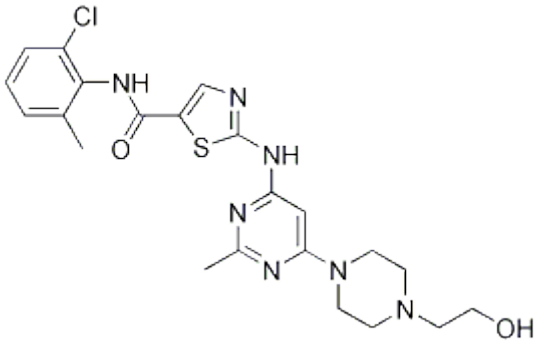

Fig. 13: Structure of dasatinib.

1.6.8. Compound 2

This molecule (**Fig. 14**) is a potent inhibitor of SFKs that interacts with ATP binding site of kinases. Compound 2 has an excellent selectivity against the receptor tyrosine and serine/threonine kinases whereas no selectivity against Src family kinases is observed, presumably due to the high sequence homology within their ATP binding sites. This compound has an IC_{50} against Fyn of 1 nM [50].

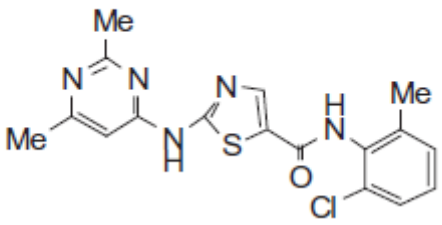

Fig. 14: Structure of compound 2.

2. Introduction to the experimental section

The design of compounds synthetized during my thesis work started with virtual screening studies that identified new Fyn inhibitors.

For this study, it was used a data set reported by Rohrer and Baumann in 2009 [51]. This data set is made up of 18 different databases of 15030 compounds (30 active and 15000 decoy molecules) for 18 different targets and among them four targeted kinase enzymes. The decoy data set for cAMP-dependent protein kinase catalytic subunit alpha (PKA) was chosen because Fyn and PKA were very similar and the binding site is highly conserved with a percentage of identity of 71%. This database contains 15020 compounds: 15000 PKA decoys and 20 selected Fyn inhibitors.

Then, a FLAP database was created by processing all templates and test compounds with the FLAP (Fingerprints for Ligands and Proteins) software, which provides ligand-based, receptor-based, and pharmacophore-based VS approaches. On this FLAP database, called Fyn-MUV, containing all the information required for calculation for each molecule, it was performed a screening by the different FLAP approaches . From this first analysis, 7564 compounds were selected and, therefore, taken into account.

Then, the filtered database was subjected to docking studies and the docked molecules were classified using two scoring functions, Chemscore from Fred and Amberscore from Dock 6.0. All the compounds that had scoring value in the range of the first 80% of the active molecules by both these scoring functions were considered to be active; 256 compounds were selected and then subjected to H-bond filter.

Analysing the X-ray complexes between Fyn and inhibitors binding the ATP binding site of the kinase, it was observed that the backbone nitrogen of M345 and the backbone oxygen of E343 and M345 were very important, since they form key hydrogen bonds with these inhibitors. All the compounds that did not form at least two H-bond interactions with these residues were rejected.

The resulting 69 compounds were then subjected to a MD (molecular dynamic) simulation to verify the stability of the inhibitor-enzyme interactions. All the ligands, that maintained the H-bonds with the backbone atoms of E343 and M345 for at least 90% of the whole MD simulation, were selected and taken into account.

These considered 36 active compounds were clustered in eight classes on the basis of their central scaffold and, for each group a representative compound was chosen (**Fig.15**).

	Compd. Structure	Code	IC_{50} (µM)[a]
VS1	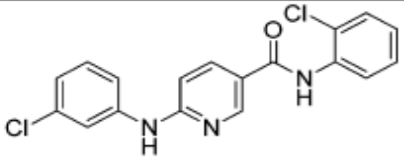	ASN 05346611	71.2
VS2	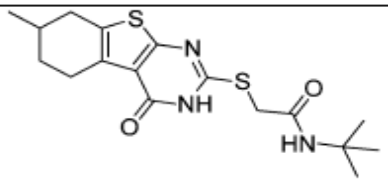	ASN 06152825	> 500
VS3	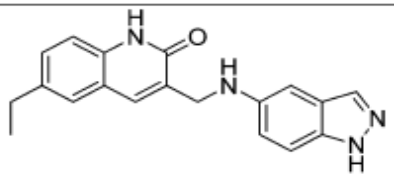	ASN 07404571	15.0
VS4	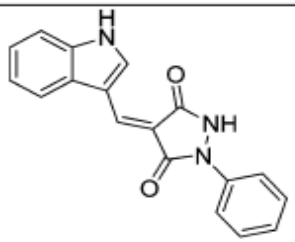	BAS 00244777	11.5
VS5	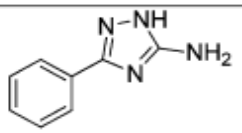	BAS 01171840	> 500
VS6	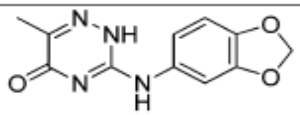	BAS 04199656	4.8
VS7	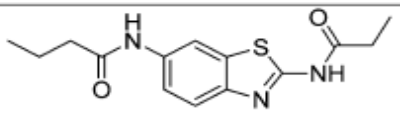	BAS 12987897	> 500
VS8	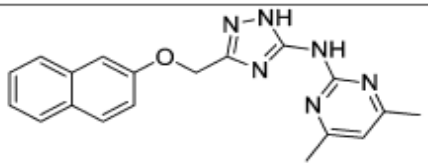	BAS 14602180	46.7
	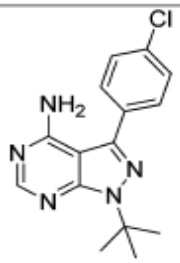	**PP2**	0.063

Fig.15 : Structures and Fyn inhibitory activities of the tested compounds.

These compounds were subjected to a Fyn inhibition assay using the reference Src inhibitor PP2 as positive control [52]. As indicated in **Fig.15**, five out of the eight compounds showed IC_{50} values ranging from 5 to 70 μM and, therefore, a good Fyn inhibitory activity.

Through the X-ray analysis of the complex inhibitor-enzyme, it was possible to observe the interactions between Fyn and the five representative compounds (**Fig.16**). With regard to compound **VS1**, the 6- aminonicotinamide central scaffold forms two H-bonds with the backbone of M345 and an H-bond with the hydroxyl group of T342; the 3-chlorophenyl ring is directed toward the solvent-accessible region of the binding site and the antipodal 2-chlorophenyl interacts with V285 and the methyl group of T342 (**Fig.16A**).

The quinolinone central scaffold of compound **VS3** forms two H-bonds with the backbone of M345 and the indazole group forms a H-bond with the nitrogen backbone of D408 and interacts with V285 and L397 (**Fig.16B**).

The pyrazolidine system of compound **VS4** forms two H-bonds with the backbone M345; the indole ring interacts with V285, L397 and forms a H-bond with the hydroxyl group of T342. Finally, the phenyl ring is direct toward the solvent-accessible region of the binding site (**Fig. 16C**).

With regard to compound **VS6**, the triazinone central scaffold interacts with the nitrogen backbone of M345 and the oxygen backbone of E343; the benzodioxole ring forms a H-bond with K299 and the amine function interacts, through a H-bond, with the hydroxyl group of T342 (**Fig. 16D**).

The triazole ring of compound **VS8** forms a H-bond with the nitrogen backbone of M345 and with the oxygen backbone of E343; the substituted 2- pyrimidinamine group interacts with V285 and with the hydroxyl group of T342 (**Fig. 16E**).

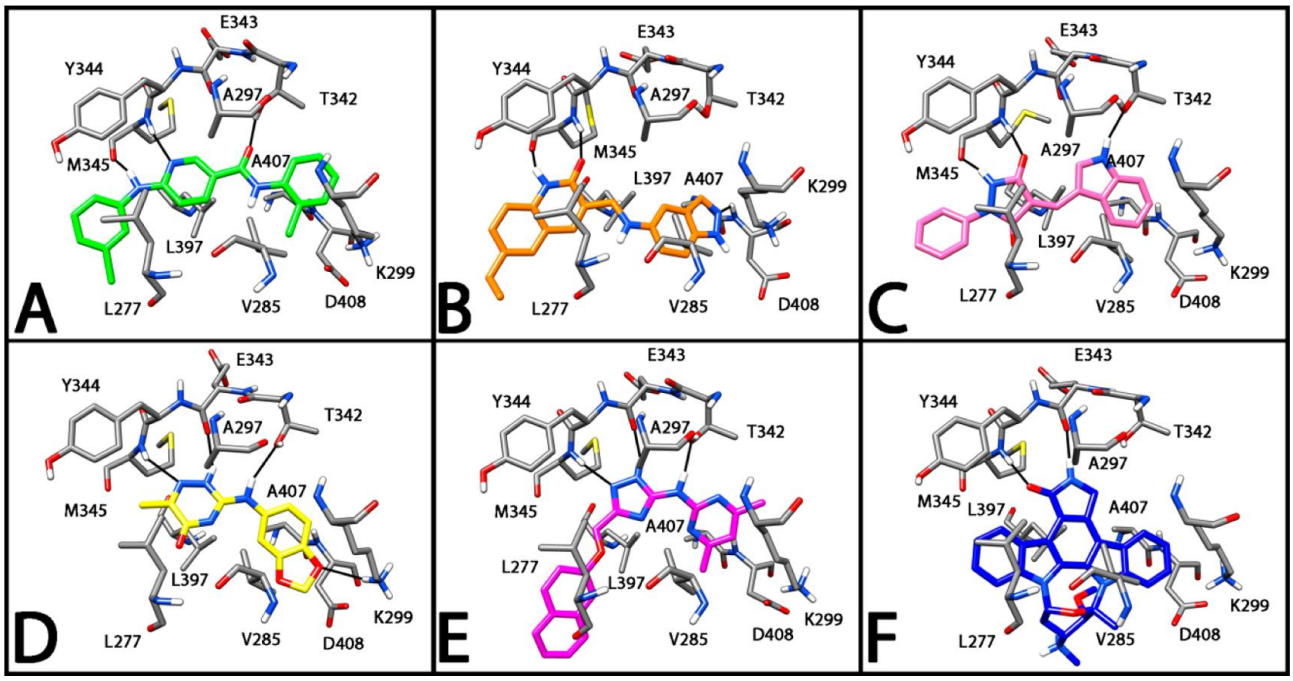

Fig.16 : Minimized average structures of compounds VS1 (A), VS3 (B), VS4 (C), VS6 (D), and VS8 (E) docked into Fyn. The X-ray complex between Fyn and staurosporine is also reported as a reference system (F).

Three of these compounds (**VS3**, **VS4** and **VS6**) were tested to evaluate their activities against different kinases. Compound **VS3** did not show any activity against the tested kinases; compounds **VS4** and **VS6** showed a moderate activity against the Epidermal Growth Factor Receptor (EGFR) (**Fig. 17**).

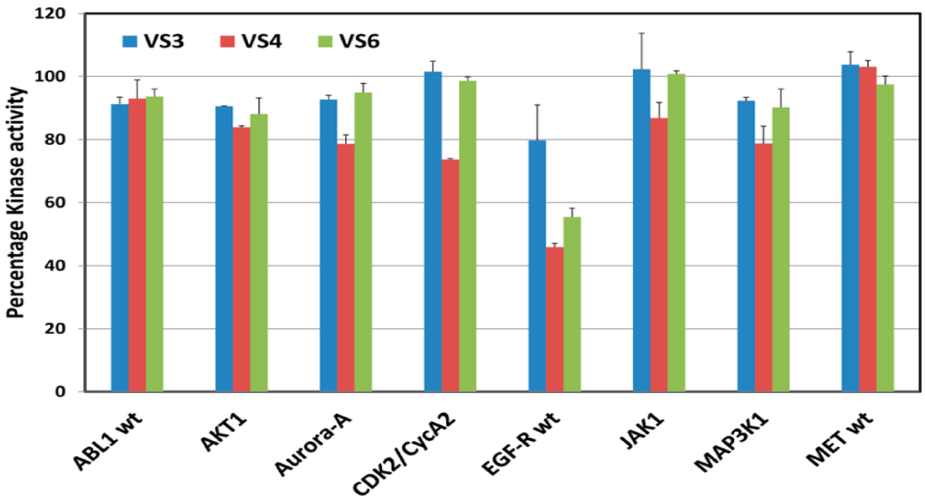

Fig. 17 : Percent kinase activity observed at 20 µM concentration of the tested compounds. Values are the average from two evaluations. Error bars indicate standard error of the mean.

Then these three compounds were tested on cell lines to evaluate their antiproliferative potency against tumour cells. The three selected cell lines were: two tumour cell lines, MDA-MB-231 (human breast carcinoma cells)and A549 (non-small cell lung cancer) and the noncancerous MRC-5 cells (human fetal lung fibroblast). All the three compounds showed good inhibitory activity against the two tumour cell lines, with IC_{50} values ranging from 63 to 198 μM. Moreover, all the compounds did not showe activity against normal cells MRC-5 (**Table. 1**).

		IC_{50} values (μM)			
cancer cell line	tissue of origin	VS3	VS4	VS6	PP2
A549	lung	117.7 ± 13.9	100.1 ± 17.5	145.0 ± 13.3	7.0 ± 1.7
MDA-MB-231	breast	136.4 ± 17.5	62.7 ± 13.1	198.2 ± 9.1	14.9 ± 4.7
MRC-5	normal fibroblast	>300	>300	>300	30.6 ± 4.0

Table 1. Cell Growth Inhibitory Activities (IC_{50}) of Compounds **VS3, VS4, VS6,** and **PP2**

3. Results and discussion

3.1. Molecular design

Considering the virtual screening studies reported in the previous chapter, it is clear that the presence of at least two hydrogen bonds between the inhibitor molecule and the binding site of Fyn kinase are necessary to inhibit the protein, and that these established interactions should be fairly stable.
In particular, some specific bonds are important:

- the H-bond with the backbone nitrogen of M345;

- the H-bond with the backbone oxygen of E343 and M345.

On the basis of the obtained results, we designed and synthesized new compounds that may be able to interact with the binding site of the enzyme and, therefore, to inhibit Fyn.
During my thesis work, seven new molecules were synthesized with the aim of improving the inhibition activity on Fyn. The design of these compounds was inspired by the structure of compound **VS6**, which, among the molecules selected during the virtual screening tests, was the one that showed the best inhibitory activity against Fyn, with an IC_{50} of 4.8 μM.
The structural modifications concern the introduction of various substituents on the two aromatic rings on the 1,2,4-triazin-5(*4H*)-one central scaffold (**Fig.18**). These compounds share the 1,2,4-triazin-5(*4H*)-one scaffold and present various groups that can behave as hydrogen-bonds acceptors such as methoxy, trifluoromethoxy, fluoro or methylenedioxy. These groups were introduced either in *para* or in *meta* position on the aromatic rings (**Fig. 19**).

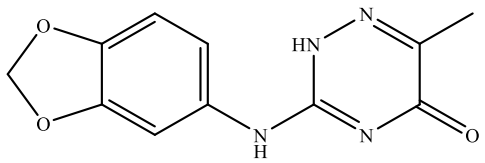

VS6

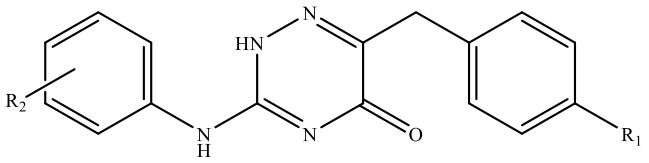

General structure of synthesized compounds

Fig. 18: Structure of **VS6** and general structure of compounds synthesized during my thesis work.

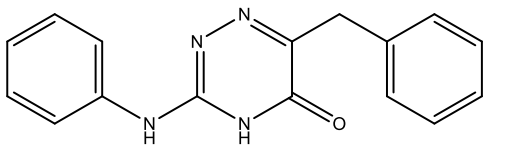

1

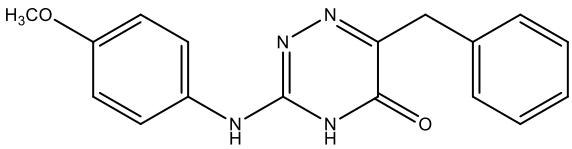

2

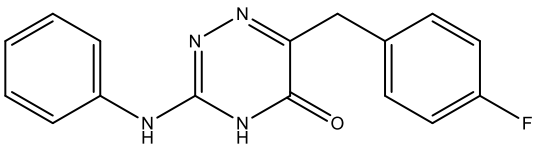

3

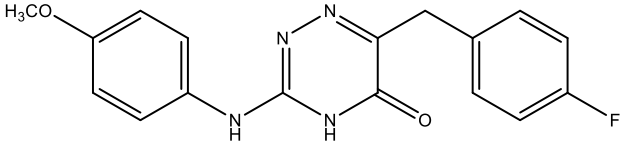

4

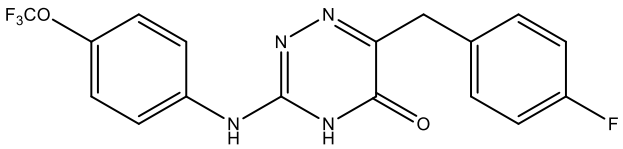

5

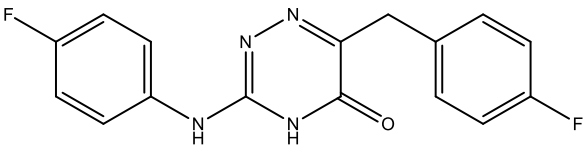

6

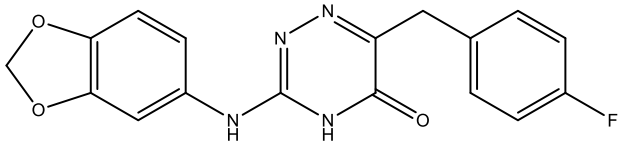

7

Fig. 19: Structures of compounds synthesized during my thesis work.

3.2. Chemical synthesis

These compounds were synthetized by adopting a previously reported synthetic strategy [53] (**Scheme 1**).

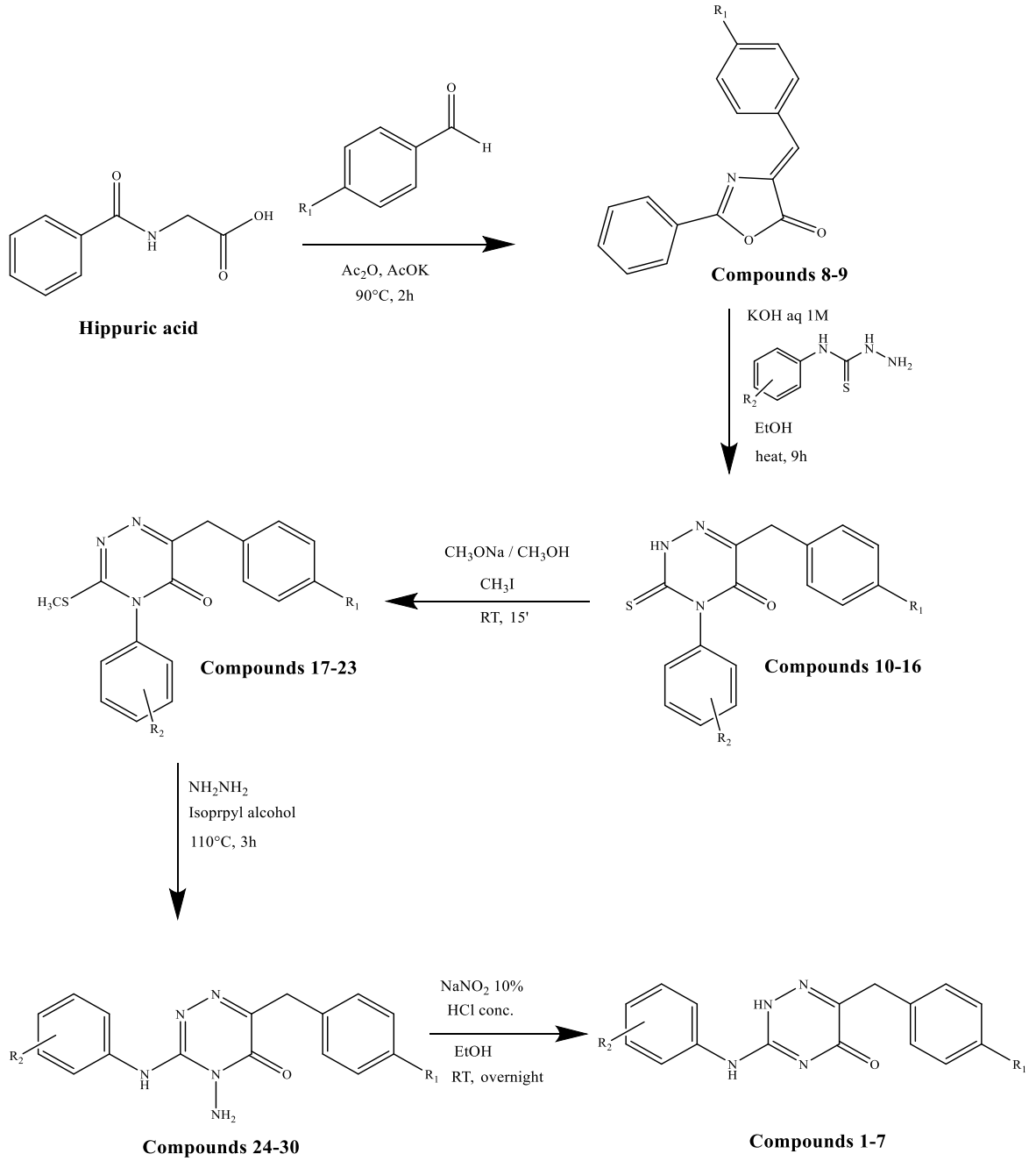

Scheme. 1: General synthesis of Fyn inhibitors.

The first step involves the formation of (*Z*)-4-benzylidene-2-phenyloxazol-5(*4H*)-one; this compound is obtained from the Erlenmeyer-Plöchl reaction, that is a cyclodehydration-condensation of the appropriate aldehyde (in this case benzaldehyde or *p*-fluorobenzaldehyde) and hippuric acid in acetic anhydride catalysed by the acetate anion of potassium acetate which was used as the base (**Scheme 2**).

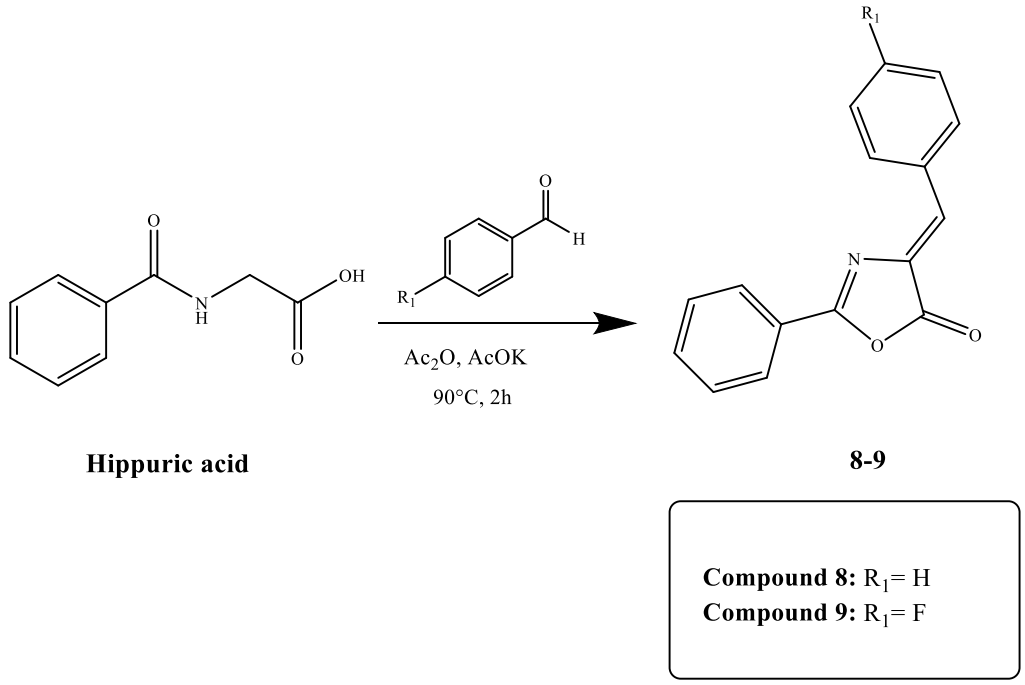

Scheme 2: Synthesis of 5-oxazolones.

In detail (**Scheme 3**) [54], the oxygen atom of hydroxyl group of hippuric acid attacks the carbonyl carbon of acetic anhydride with the elimination of a molecule of acetic acid. After keto-enol tautomerism, a further attack of compound **c** on the aromatic aldehyde takes place, in such a way that compound **d** is obtained. Subsequently, a molecule of water is eliminated and a new keto-enolic equilibrium is formed; the enol form (compound **f**) gives cyclization obtaining compound **g**. In the last step, a molecule of acetic acid is eliminated and the desired oxazolone is formed (compound **8** or **9**).

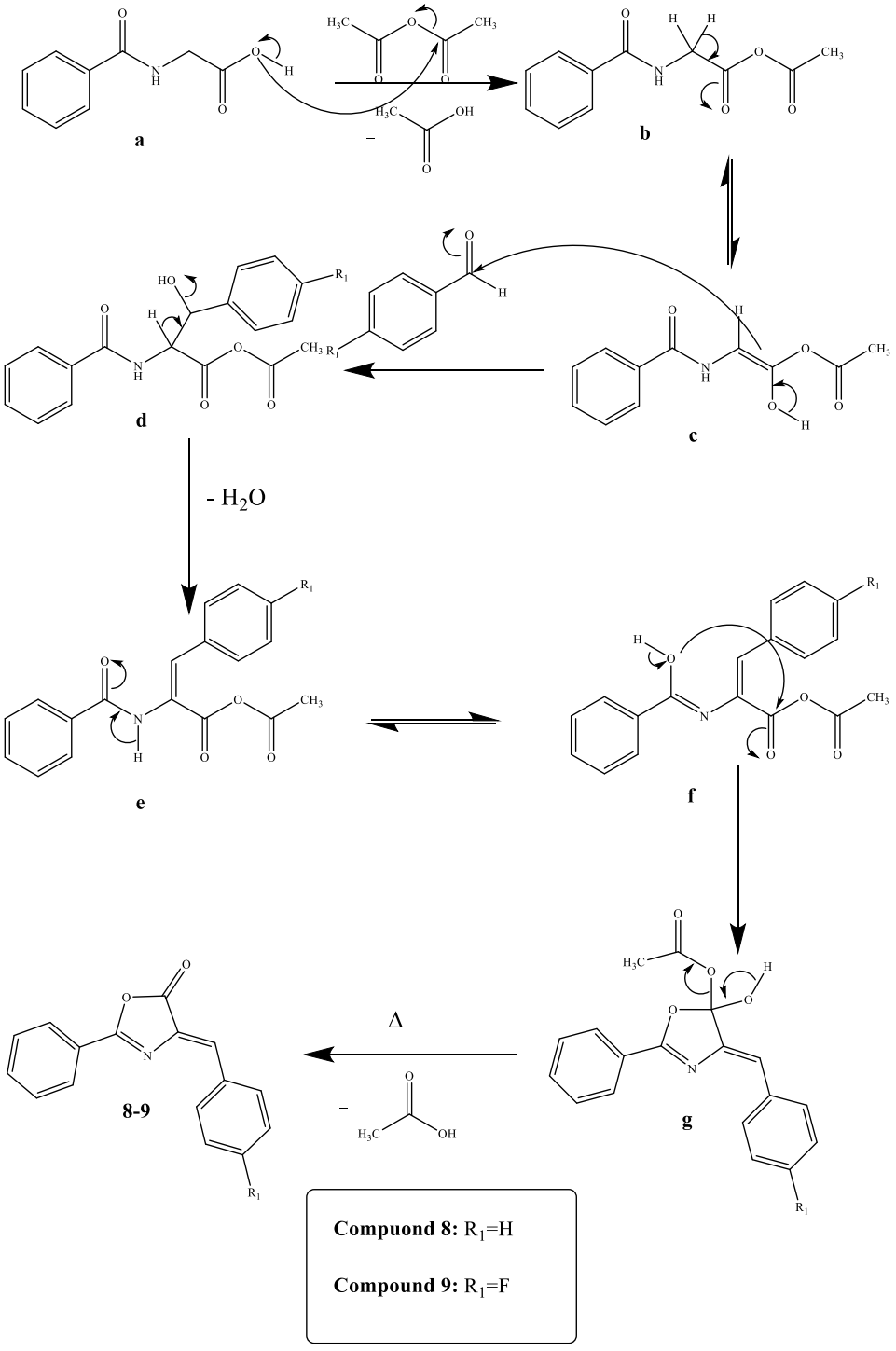

Scheme 3: Mechanism of Erlenmeyer-Plöchl reaction.

Initially, the crude compound was purified through a chromatographic column, using as eluent, a mixture of *n*-hexane and AcOEt; in this way, we were able to separate the reaction product from the unreacted benzaldehyde. Because the obtained product needed large volume of solvents to be completely eluted, we tried to purify this product by simply washing the crude precipitate with distilled hexane to remove the

starting material benzaldehyde. This method proved to be efficacious since it was possible to get the pure product with comparable yields, optimizing the working time and solvent consumption/disposal.

The second step of the synthetic strategy (**Scheme 4**) is divided into two parts.

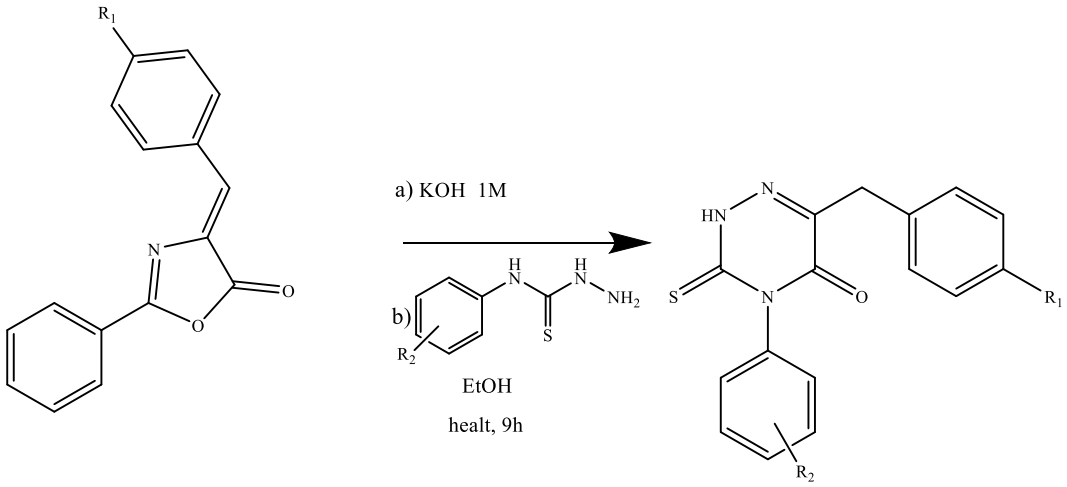

8-9

10-16

Compuond 8 : R_1=H

Compound 9 : R_1=F

Compound 10 : R_1= H, R_2=H
Compound 11 : R_1= H, R_2= *p*-OCH_3
Compound 12 : R_1= F, R_2= H
Compound 13 : R_1= F, R_2= *p*-OCH_3
Compound 14 : R_1= F, R_2= *p*-OCF_3
Compound 15 : R_1= F, R_2= *p*-F
Compound 16 : R_1= F, R_2= 3,4-OCH_2O-

Scheme 4: The second step of the synthetic strategy

In the first part, the oxazolone reacts with aqueous KOH; in this way, the lactone ring is opened with the anion formation of the corresponding hydroxy acid (compound **b**) which is in keto-enolic equilibrium with compound **c** (**Scheme 5**). The amide bond of compound **d** is then hydrolyzed with formation of compound **e**; the latter is in keto-

enolic equilibrium with compound **f**. The subsequent hydrolysis of the imine group leads to the formation of compound **h**.

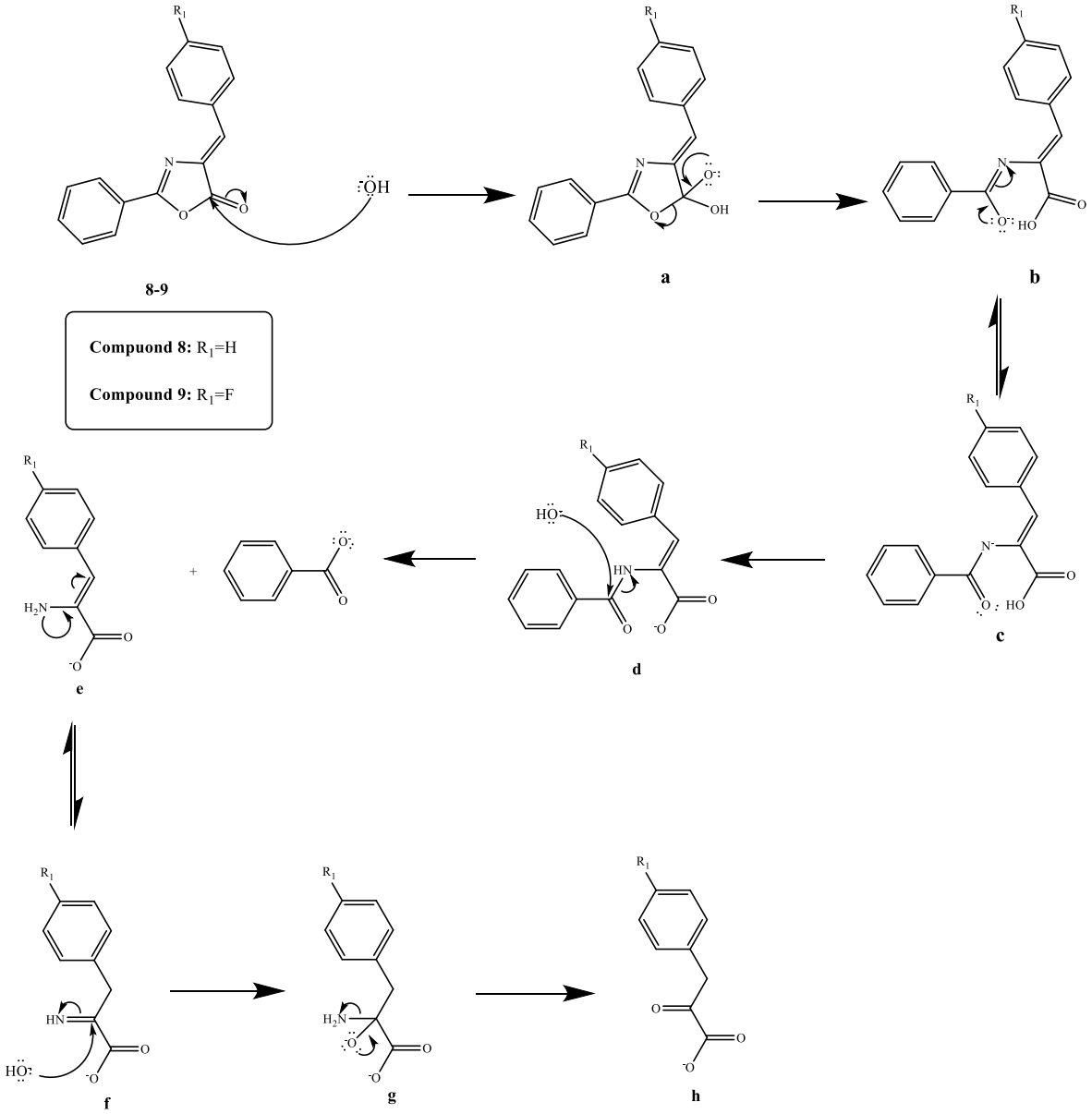

Scheme 5: Base-catalyzed hydrolysis of oxazolones.

After the acidification with acetic acid, in the second part of this step, the formed intermediate reacts with variously substituted 4-aryl thiosemicarbazide. In detail (**Scheme 6**), compound **h** is protonated by acetic acid forming compound **i**, an α keto acid which reacts with 4-arylthiosemicarbazide; in this way compound **l** is formed.

Subsequently, two water molecules are released by the cyclization of compound **m** and formation of compounds **10-16**.

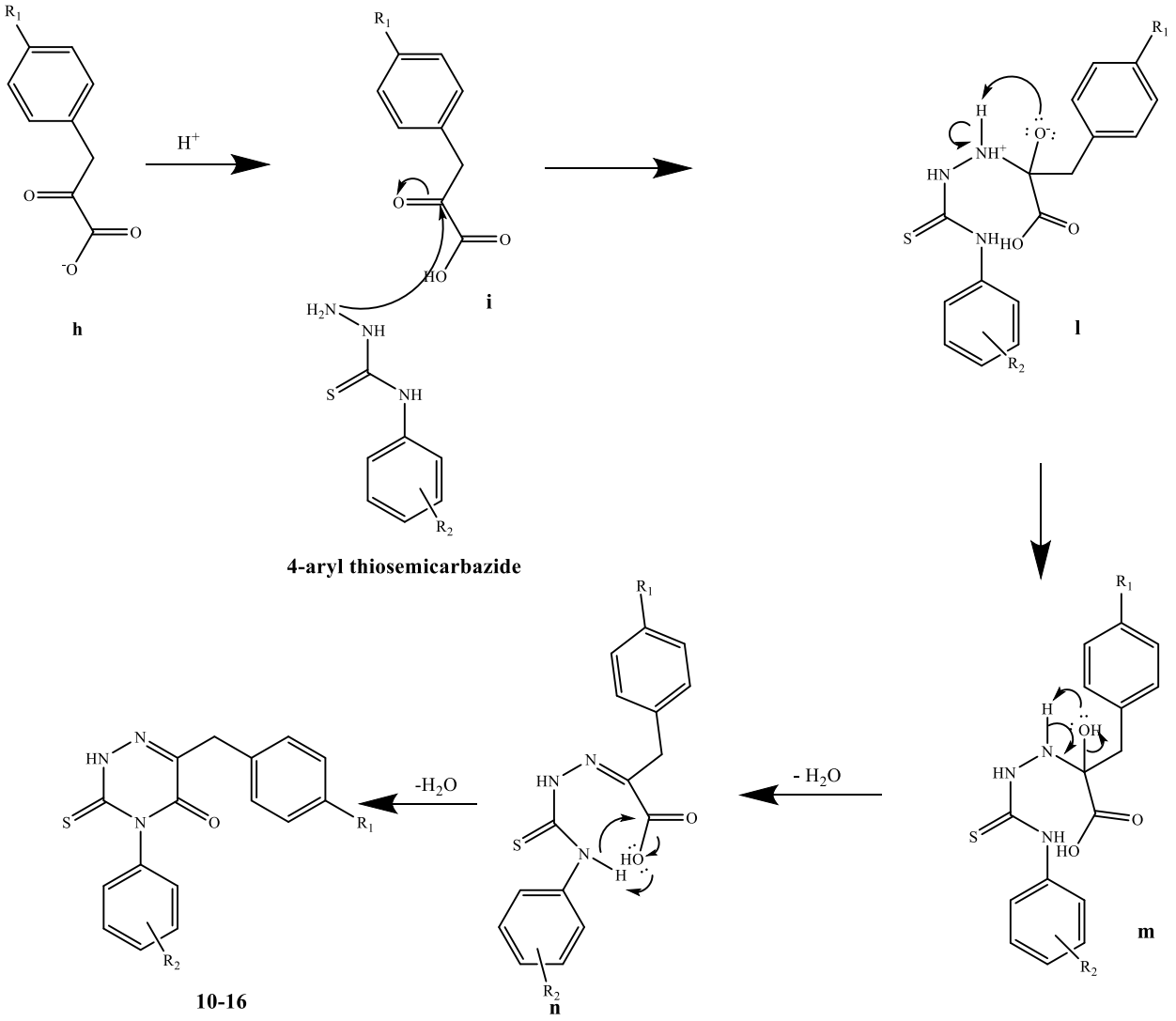

Compound 10 : R_1= H, R_2=H
Compound 11 : R_1= H, R_2= *p*-OCH_3
Compound 12 : R_1= F, R_2= H
Compound 13 : R_1= F, R_2= *p*-OCH_3
Compound 14 : R_1= F, R_2= *p*-OCF_3
Compound 15 : R_1= F, R_2= *p*-F
Compound 16 : R_1= F, R_2= 3,4-OCH_2O-

Scheme 6: Formation of compounds **10-16** from intermediate **m** with variously substituted 4-arylthiosemicarbazides.

Scheme 7 shows the subsequent methylation of the compounds **10-16** with CH_3I in CH_3ONa/CH_3OH.

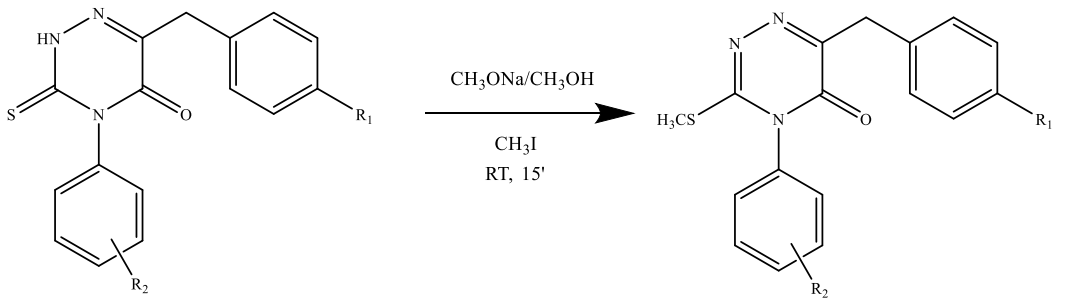

10-16 **17-23**

Compound 10 : R_1= H, R_2=H
Compound 11 : R_1= H, R_2= *p*-OCH_3
Compound 12 : R_1= F, R_2= H
Compound 13 : R_1= F, R_2= *p*-OCH_3
Compound 14 : R_1= F, R_2= *p*-OCF_3
Compound 15 : R_1= F, R_2= *p*-F
Compound 16 : R_1= F, R_2= 3,4-OCH_2O-

Compound 17 : R_1=H, R_2=H
Compound 18 : R_1=H, R_2=*p*-OCH_3
Compound 19 : R_1=F, R_2=H
Compound 20 : R_1=F, R_2=*p*-OCH_3
Compound 21 : R_1=F, R_2=*p*-OCF_3
Compound 22 : R_1=F, R_2=*p*-F
Compound 23 : R_1=F, R_2=3,4-OCH_2O-

Scheme 7: Methylation of compounds **10-16**.

This reaction was monitored by thin-layer chromatographic (TLC) and it was observed the formation of two reaction products with slightly different R_f (retention factor).

The two compounds, **1** and **2**, were separated and isolated by a chromatographic column, using as eluent a mixture of *n*-hexane and AcOEt, and subsequently they were analysed by ^{1}H-NMR spectroscopy. The two spectra were very similar, differing only in the singlet position due to CH_3 (2.54 ppm in the spectrum of compound **1** and 4.00 ppm in that of compound **2**). The two compounds were produced with comparable yields and, given the short duration of the reaction (only 15 minutes), probably they formed simultaneously.

We have proposed three possible structures of the two reaction compounds (**Fig.20**).

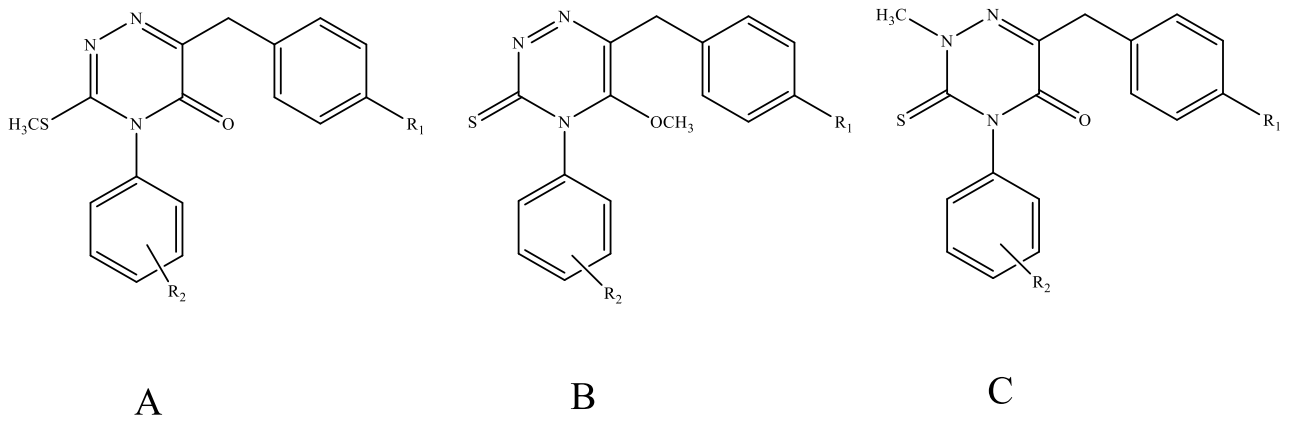

Fig. 20: Possible structures of compounds formed during methylation.

Compound **A**, in which the sulphur atom is methylated, is the desired compound; in the compound **B**, the oxygen atom is methylated and in the compound **C** methylation occurs on the nitrogen atom.

In order to confirm the hypothesized structures, the two compounds were also analysed by IR spectroscopy (**Fig. 21**). By means of this analysis we hoped to observe the obvious differences between the spectra, such as the absence of the peak due to stretching the C=O group if one of the two compound, **1** or **2**, was methylated on carbonyl oxygen (structure **B**). Strong IR absorptions at 1680-1690 cm^{-1} were present in both compounds, thus suggesting that they are more likely represented by structures **A** and **C** (**Fig. 20**).

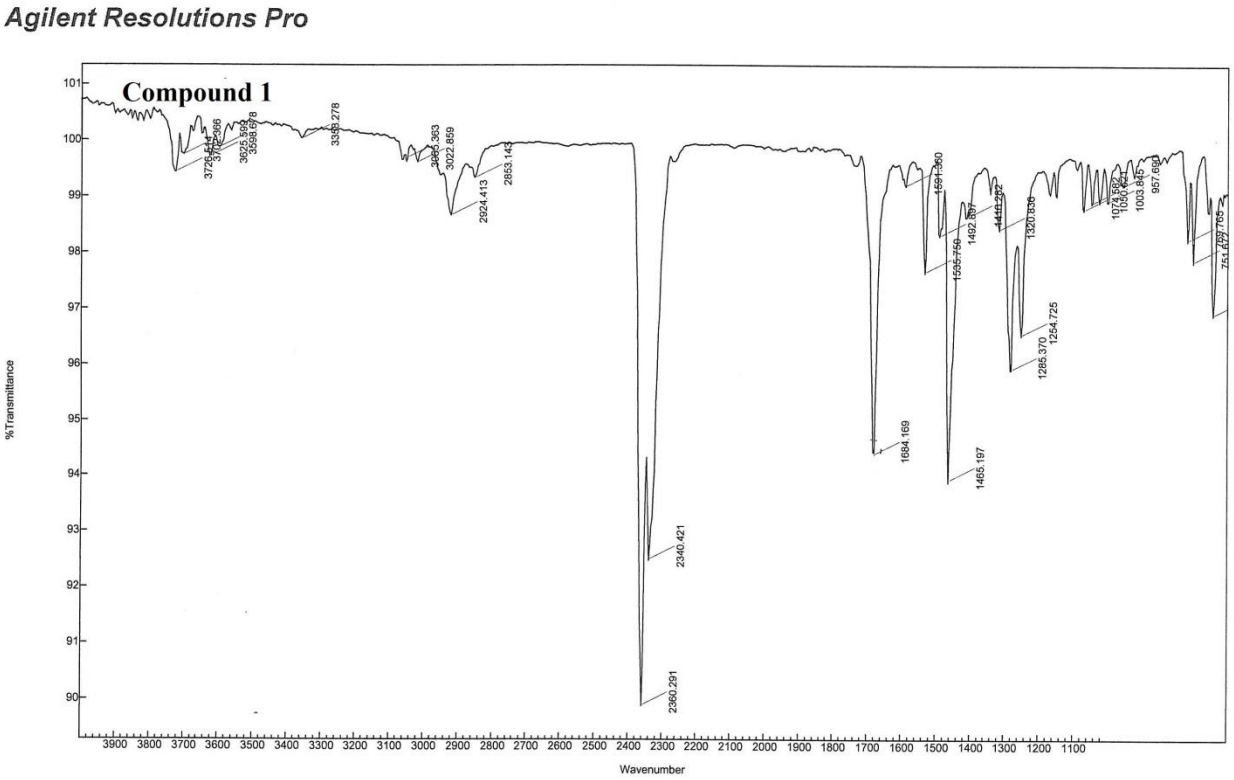

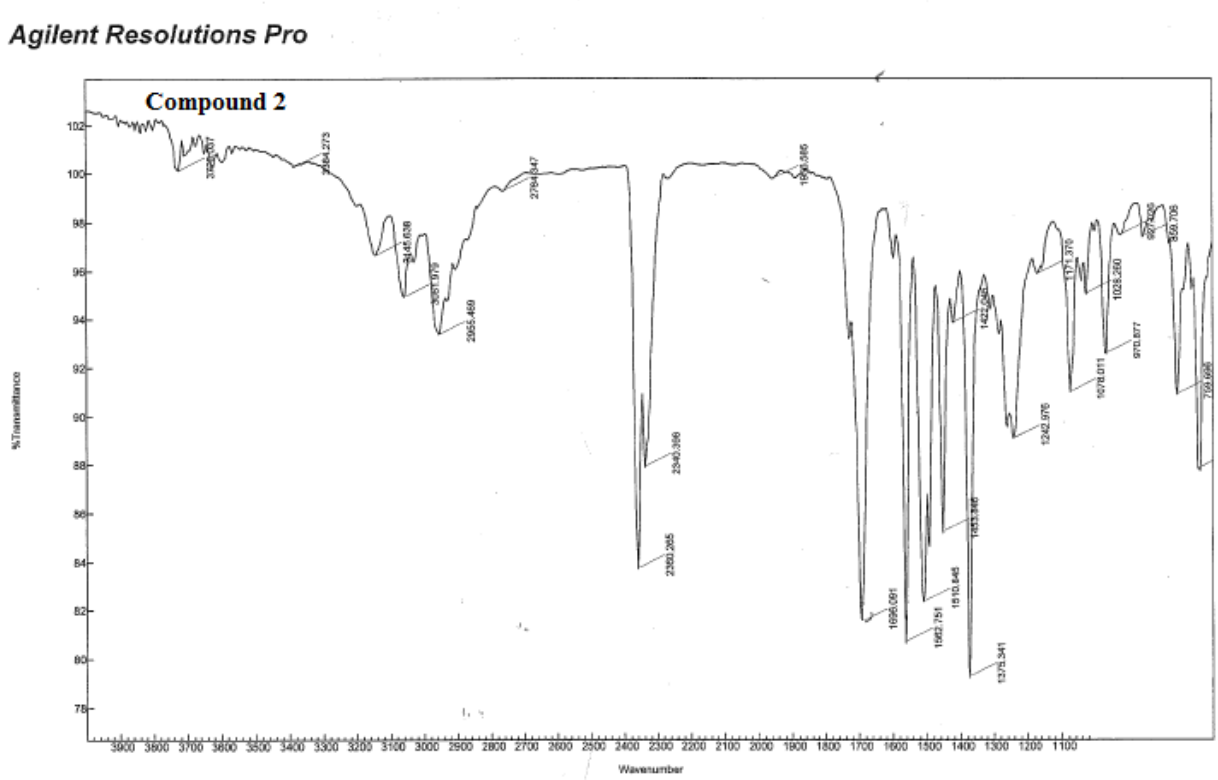

Fig. 21: IR spectra of the products of the methylation.

Both the isolated compounds were reacted with hydrazine in isopropanol, in the next step of the synthetic strategy (**Scheme 8**).

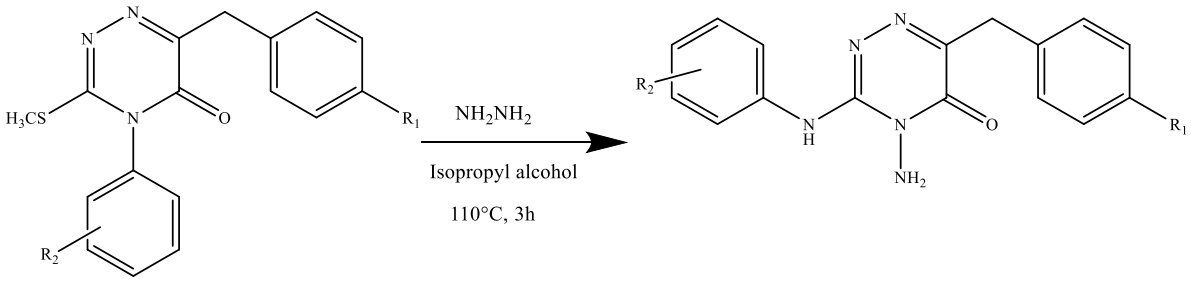

17-23 **24-30**

Compound 17 : R_1=H, R_2=H
Compound 18 : R_1=H, R_2=*p*-OCH_3
Compound 19 : R_1=F, R_2=H
Compound 20 : R_1=F, R_2=*p*-OCH_3
Compound 21 : R_1=F, R_2=*p*-OCF_3
Compound 22 : R_1=F, R_2=*p*-F
Compound 23 : R_1=F, R_2=3,4-OCH_2O-

Compound 24 : R_1=H, R_2=H
Compound 25 : R_1=H, R_2=*p*-OCH_3
Compound 26 : R_1=F, R_2=H
Compound 27 : R_1=F, R_2=*p*-OCH_3
Compound 28 : R_1=F, R_2=*p*-OCF_3
Compound 29 : R_1=F, R_2=*p*-F
Compound 30 : R_1=F, R_2=3,4-OCH_2O-

Scheme 8: Reaction of compounds **17-23** with hydrazine in Isopropyl alcohol.

We expected that only one of the two compounds could react (structure **A**), giving the formation of the desired product.

The products obtained from these two parallel reactions were independently analysed by ^{1}H-NMR spectroscopy and we observed that the two spectra coincided. Both the compounds, therefore, reacted with hydrazine forming the same product (**Fig.22**).

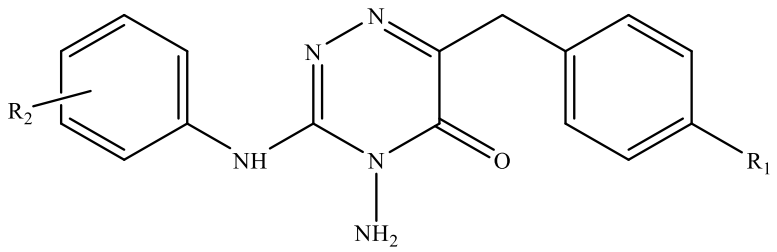

Fig. 22: General structure obtained by the reaction of compound **1** and **2** with hydrazine in isopropanol.

The **Scheme 8** shows the conditions under which this reaction occurs. In this case, compounds **17-23** were submitted to a rearrangement step in the presence of hydrazine in isopropanol to get derivatives **24-30**.

In the next step, that is the final step of synthetic strategy, the compounds **24-30** were reacted with $NaNO_2$ and concentrated hydrochloric acid in EtOH. (**Scheme 9**)

It is a reaction of deamination with N_2 release and formation of the final compounds **1- 7**.

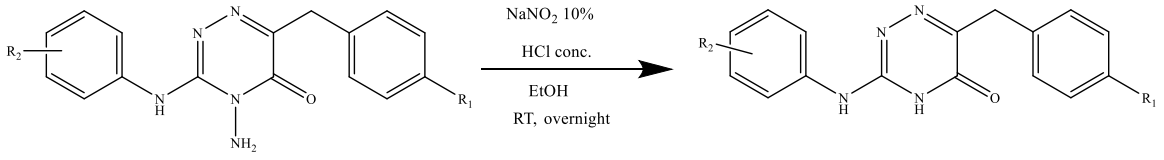

24-30 **1- 7**

Compound 24 : R_1=H, R_2=H
Compound 25 : R_1=H, R_2=*p*-OCH_3
Compound 26 : R_1=F, R_2=H
Compound 27 : R_1=F, R_2=*p*-OCH_3
Compound 28 : R_1=F, R_2=*p*-OCF_3
Compound 29 : R_1=F, R_2=*p*-F
Compound 30 : R_1=F, R_2=3,4-OCH_2O-

Compound 1 : R_1=H, R_2=H
Compound 2 : R_1=H, R_2=*p*-OCH_3
Compound 3 : R_1=F, R_2=H
Compound 4 : R_1=F, R_2=*p*-OCH_3
Compound 5 : R_1=F, R_2=*p*-OCF_3
Compound 6 : R_1=F, R_2=*p*-F
Compound 7 : R_1=F, R_2=3,4-OCH_2O-

Scheme 9: Final step of the synthesis.

During my work in the laboratory, I also synthetized hippuric acid (starting compound of the synthetic strategy) and the differently substituted 4-phenyl thiosemicarbazides, necessary in the second step of the synthetic route, that were not commercially available.

For the synthesis of hippuric acid (benzoyl glycine), glycine is reacted with benzoyl chloride in the presence of NaOH 10% (**Scheme 10**).

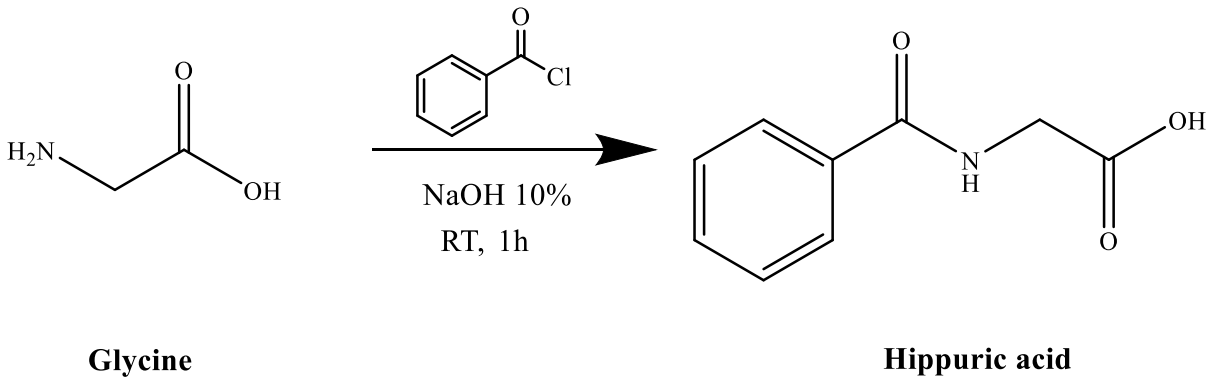

Scheme 10: Synthesis of Hippuric acid.

This reaction is known as "Schotten-Baumann" reaction and the mechanism is shown in **Scheme 11**.

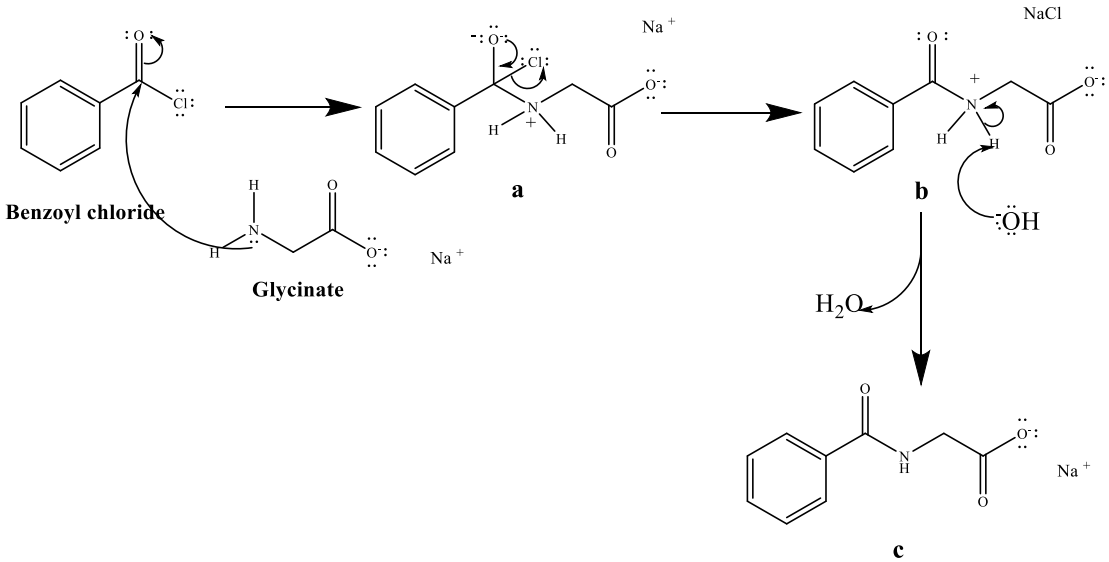

Scheme 11: Mechanism of reaction of the Schotten – Baumann reaction.

The Schotten-Baumann reaction is an reaction used to convert an acyl halide to an amide if reacted with an amine and base. The reaction begins with the nitrogen attacking the carbonyl carbon of the acyl halide which rearranges eliminating the chlorine atom. Deprotonation by the base then provides the final amide product (compound **c**).

In our case, the reaction product is then acidified with concentrated hydrochloric acid to protonate the carboxylic acid group and the hippuric acid is obtained.

Finally, for the synthesis of variously substituted 4-phenyl thiosemicarbazides (which were required in the second step of the synthetic pathway), the corresponding isothiocyanate was reacted with hydrazine in the presence of isopropanol (**Scheme 12**). It is a reaction rather fast because the duration is of just one hour.

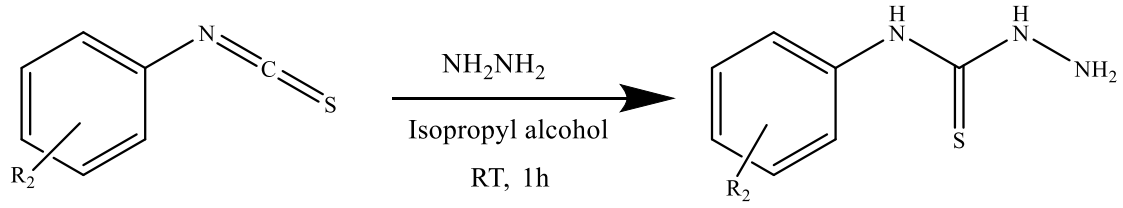

31-35 **36-40**

Compound 31 : R_2=H
Compound 32 : R_2=*p*-OCH_3
Compound 33 : R_2=*p*-OCF_3
Compound 34 : R_2=*p*-F
Compound 35 : R_2=3,4-OCH_2O-

Compound 36 : R_2=H
Compound 37: R_2=*p*-OCH_3
Compound 38 : R_2=*p*-OCF_3
Compound 39 : R_2=*p*-F
Compound 40 : R_2=3,4-OCH_2O-

Scheme 12: Synthesis of variously substituted 4-phenyl thiosemicarbazides.

For the synthesis of compound **40**, the starting isothiocyanate was not commercially available, thus it was synthesized starting from 3,4-methylenedioxy aniline.

Aniline is reacted with CS_2 and Et_3N in the presence of di-*tert*-butyl dicarbonate (Boc_2O) and 4-dimethylaminopyridine (DMAP) in EtOH (**Scheme 13**).

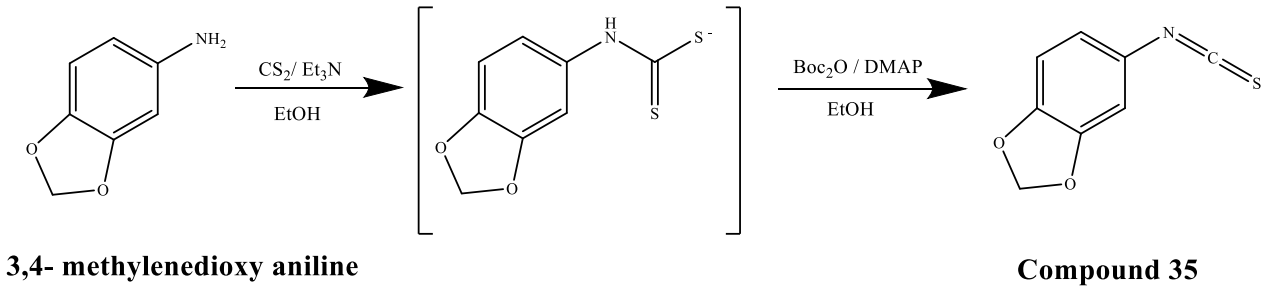

3,4- methylenedioxy aniline **Compound 35**

Scheme 13: Synthesis of 3,4-methylenedioxy isothiocynate

As shown in the **Scheme 14** [55], initially aniline reacts with CS_2 forming the dithiocarbamate, which in a second moment, reacts with Boc_2O to form CO_2 and an unstable adduct that rapidly decomposes giving isothiocyanate **35**.

The presence of triethylamine is necessary for the stabilisation and complete formation of the dithiocarbamate.

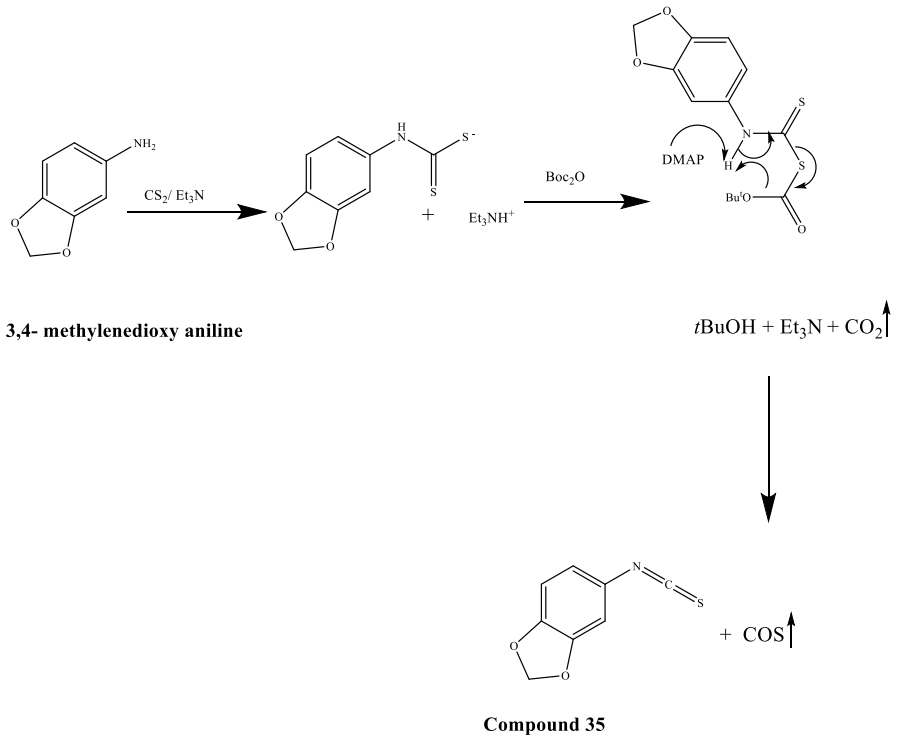

3,4- methylenedioxy aniline

Compound 35

Scheme 14: Mechanism for the base-catalysed synthesis of isothiocyanates from the corresponding amines using di-*tert*-butyl dicarbonate.

The compound **35**, as is shown in the **Scheme 12**, is reacted with hydrazine in isopropanol, thus obtaining the desired thiosemicarbazide (Compound **40**).

During my thesis work, I tried to synthetize also a series of compounds in which the starting compound was the oxazolone bearing a methyl group on the exocyclic double bond, resulting from reaction of hippuric acid and acetaldehyde on the condition of the Erlenmeyer-Plöchl reaction. (**Scheme 15**)

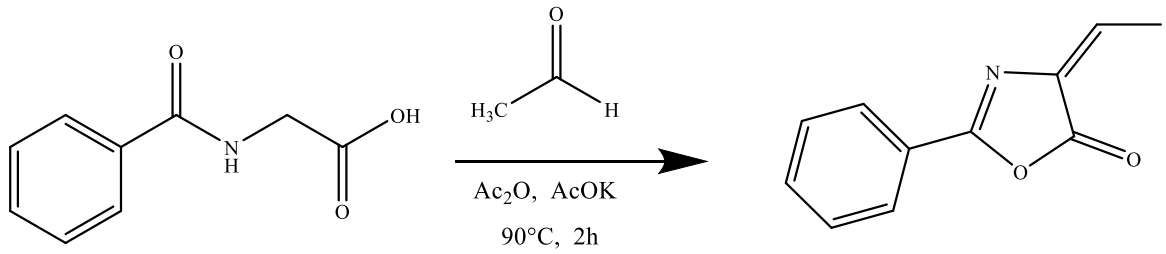

Hippuric acid **Compound 41**

Scheme 15: Erlenmeyer- Plöchl reaction with acetaldehyde.

This reaction was repeated several times; the first time, we performed a classic reaction work-up with water and AcOEt and then all the various products present in the reaction mixture were isolated, using a chromatographic column. These compounds were analysed by ^{1}H-NMR spectrometry and we did not obtain the desired product (compound **41**).

In another attempt, I added EtOH to the reaction mixture, it formed an orange precipitate which was then filtered and analyzed by ^{1}H-NMR spectrometry, but unfortunately it did not correspond to the desired compound.

At present, the reasons why this reaction was not successful were not further investigated.

In the last part of my thesis work, I synthetized on a large scale compounds**1** and **24** (**Fig. 23**) to perform a crystallization on the pure products. These two compounds

were selected considering the good total yield of the synthesis of compound **1** (21 %), compared to the other synthesized compounds (7-18 %).

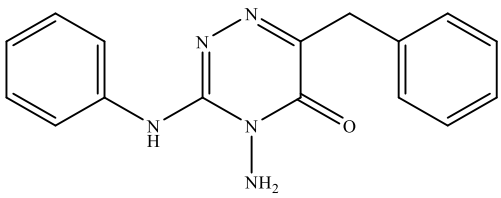

Compound 24

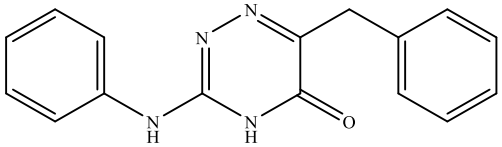

Compound 1

Fig. 23: Structure of crystallized compounds.

The crystallization of compound **24** was conducted in $CHCl_3$. The compound was dissolved in a minimum volume of hot $CHCl_3$ and then the obtained solution was cooled slowly.

In the other case, compound **1** was dissolved in a minimal amount of hot AcOEt and then, the flask containing the solution was placed in a container in which it was present hexane.

In both cases, I obtained white crystalline aggregates in which the single crystals were aggregated in radial disposition (**Fig. 24**).

These crystals will be subjected to X-ray analysis in order to confirm their structures.

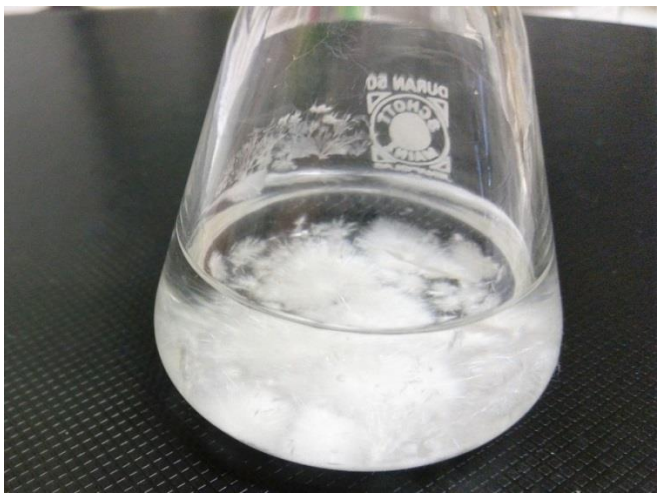

Fig.24: Crystalline aggregates obtained from the crystallization of compound **1**.

4. Summary and conclusions

Fyn is a non-receptor tyrosine kinase, belonging to the Src family kinases (SFKs).
This protein plays a key role in several transduction pathways in physiological and pathological situations. Fyn is implicated in brain development processes, such as myelination, differentiation of oligodendrocytes and synapses formation. Several lines of evidence implicate Fyn in the Alzheimer's disease (AD) and other tauopathies. In fact, Fyn phosphorylates Tau protein (a microtubule-associated protein) at Tyr18. Tyrosine-phosphorylated Tau is one of the main components present in the tangles that are characteristic of AD brain. Moreover, Fyn mediates Aβ-induced synaptic deficit and neurotoxicity and is activated by Aβ oligomers, causing synaptic and cognitive impairment.
Fyn also takes part in numerous cellular functions such as growth and cell proliferation, morphogenesis and cell motility. Fyn overexpression determines an increase in cell growth, cell proliferation and cell motility favouring the formation and development of cancer and metastasis.
Since Fyn overexpression is widely involved in many diseases, this protein is an important pharmaceutical target taken into account especially for the treatment of neurodegenerative diseases and cancers.
Although there are not selective inhibitors for Fyn in the literature, several molecules, such as staurosporine, PP1 and PP2, dasatinib and saracatinib, are known to be able to inhibit this protein by interacting with its catalytic site..
Virtual screening studies showed that key-interactions with two residues (E343 and M345), which are present in the catalytic site of this kinase, are required to have a good inhibitory activity.
During my thesis work, I have synthesized seven molecules that share the same 1,2,4-triazin-5-(*2H*)-one scaffold, differing for some substitutions in the aryl rings (R_1 and

R_2, **Fig.25**). The design of these compounds was inspired from the structure of a compound identified as a good Fyn inhibitor by virtual screening studies.

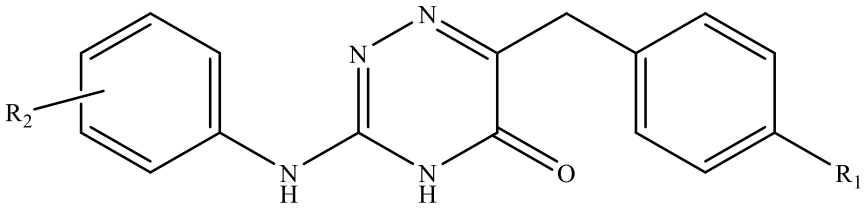

Fig.25: General structure of the synthesized compounds

The first step of the synthetic strategy was the reaction of an appropriate aldehyde (benzaldehyde or *p*-fluorobenzaldehyde) with hippuric acid in acetic anhydride and in presence of potassium acetate (Erlenmeyer-Plöchl reaction). This step led to the formation of (*Z*)-4-benzylidene-2-phenyloxazol-5(*4H*)-one. In the second step, oxazolone was submitted to a base-catalysed hydrolysis and then, the formed intermediate reacted with variously substituted 4-phenyl thiosemicarbazides. The compounds obtained in this step were then methylated with CH_3I in CH_3ONa/ CH_3OH and subsequently, the products of methylation were submitted to a rearrangement in presence of hydrazine in isopropanol alcohol. The final step was a deamination in presence of $NaNO_2$ and concentrated hydrochloric acid in EtOH. This reaction led to the formation of final compounds.

The final products are currently being evaluated for Fyn inhibitory activity. These assays will determine which are the compounds with the best inhibitory activity against Fyn, and therefore, the substituents which best interact with the binding site of the protein.

Considering studies of molecular modelling conducted on the molecule that has inspired the structure of the compounds synthesized during my thesis work (**VS6**), it was observed that this molecule, in addition to its interaction with E343 and M345,

also forms a H-bond with K299. In the formation of this bond, the benzodioxole ring of **VS6** behaves as an H bond acceptor. Therefore,once the screening results will be available for this first series of compounds, this project will continue with the synthesis of a new series of compounds containing the R_2 substituent that will prove to be the most suitable H bond acceptor, together with a differentiation in position 5, where variously substituted aryl or heteroaromatic rings can be linked to the central scaffold by a methylene or a –NH- moiety (**Fig.26**).

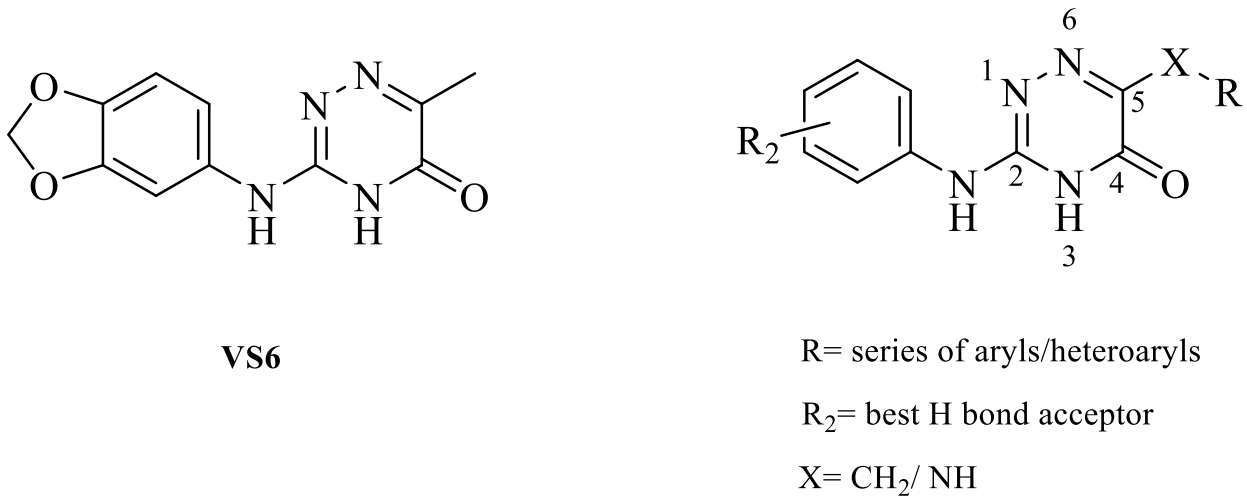

Fig.26: VS6 and general structures of the hypothesized compounds for the future project

5. Experimental procedures

Materials and methods

All reactions performed during my thesis work were monitored by thin-layer chromatographic (TLC) using Merck aluminium silica gel (60 F254) sheets which were observed under a UV lamp (254 nm).

Anhydrous sodium sulfate was used to dry the organic phases obtained from treatment of various reactions.

Crude compounds were purified by column chromatography that was performed using silica gel 60 (0.040- 0.063 mm; Merck).

Finally, to confirm the structure of all the reaction intermediates and final products it was used nuclear magnetic resonance spectrometry; NMR spectra were obtained with a Bruker Avance III HD operating at 400 Hz and relative to the solvent signal. Chemical shifts are reported in parts per million (ppm) and coupling constants (J) in Hz. The multiplicities were explained using the following abbreviations: s = singlet, d = doublet, m = multiplet, q = quartet, dd = double doublet, tt = triple triplet, bs = broad singlet.

Hippuric acid

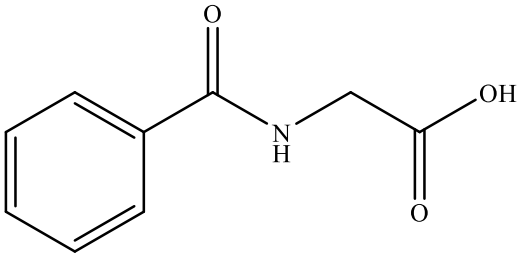

benzoylglycine

Benzoyl chloride (1.8 ml, 15.3 mmol) was added to a solution of glycine (1000 mg, 13.32 mmol) in NaOH 10% (9.99 ml) in a single-neck round bottom flask. The mixture was stirred at room temperature for 1h and it formed a white precipitate.

The reaction product was poured in a beaker containing ice and then was acidified with HCl conc. . The crude product was filtered, washed with $CHCl_3$ and cold water and dried under reduced pressure. It was obtained a white solid (hippuric acid, 1.854 g, 10.35 mmol) with a yield of 78 %.

^{1}H NMR (DMSO-d_6) δ ppm:

3.92 (d, 2H, J= 5.9; 7.46- 7.51 (m, 2H); 7.54 (tt; 1H, J= 7.3, 1.3); 7.87 (AA'XX', 2H, J_{AX}= 8.2, $J_{AA'/XX'}$= 1.8); 8.83 (t, 1H, J= 5.8)

8

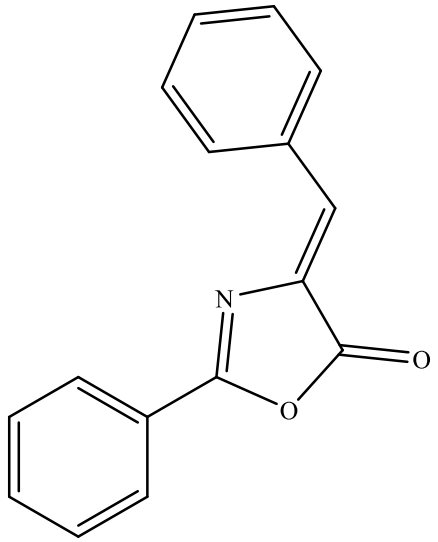

(*Z*)-4-benzylidene-2-phenyloxazol-5(4*H*)-one

Under argon atmosphere, benzaldehyde (0.96 ml, 9.42 mmol), acetic anhydride (2.66 ml 28.26 mmol), hippuric acid (1.688 g, 9.42 mmol) and potassium acetate (924.6 mg, 9.42 mmol) were inserted in a flame-dried double-necked round flask. After adding potassium acetate, it formed an orange solution. The mixture was refluxed at 90 °C for 2 h. After cooling at RT, the crude mixture was extracted with AcOEt. The organic phase was dried and concentrated. The crude product was purified with chromatography column in silica gel (*n*-Hexane/ AcOEt 95:5) to afford compound **8** (1.830 g, 7.34 mmol) as yellow, voluminous solid with a yield of 78%.

^{1}H NMR ($CDCl_3$) δ (ppm):

7.27(s, 1H); 7.45-7.57 (m, 5H); 7.62 (tt, 1H, *J*= 7.4, 1.4 Hz); 8.19-8.23 (m, 4H)

10

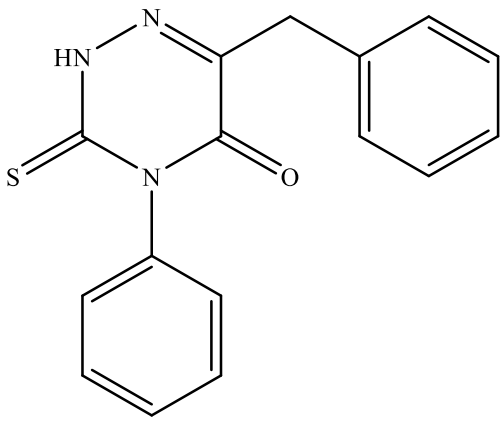

6-benzyl-4-phenyl-3-thioxo-3,4-dihydro-1,2,4-triazin-5(2*H*)-one

To the compound **8** (500 mg, 2.01 mmol) in a two-necked round bottomed flask, a solution of KOH 1M (6.03 ml, 6.03 mmol) was added. The mixture was refluxed at 115 °C for 4 h. After cooling at room temperature, it was acidified, in an ice bath, with acetic acid. Then 4-phenyl-thiosemicarbazide (335.3 mg, 2.01 mmol) in EtOH (6.03ml) was added. The resulting solution was stirred and refluxed at 105 °C for 5h. The reaction mixture was extracted with AcOEt. The organic phase was dried and evaporated under reduced pressure. The crude product was purified by a column chromatography in silica gel (*n*-Hexane / AcOEt 85:15) to afford compound **10** (286.8 mg, 0.97 mmol) as a white/ yellow solid with a yield of 48%.

^{1}H NMR ($CDCl_3$) δ ppm:

3.98 (s, 2H); 7.18-7.21 (m, 2H); 7.27- 7.37 (m, 5H); 7.46-7.55 (m, 3H); 10.31 (bs, 1H)

17

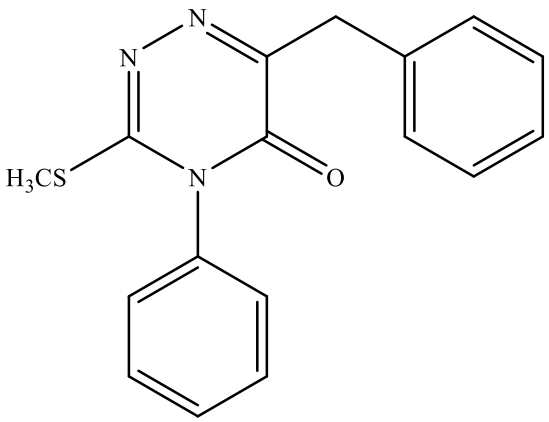

6-benzyl-3-(methylthio)-4-phenyl-1,2,4-triazin-5(4*H*)-one

A solution of compound **10** (100 mg, 0.338 mmol) in CH_3OH (0.4 ml) under argon was cooled and treated with a solution of CH_3ONa/CH_3OH (0.08 ml, 0.338 mmol). Then CH_3I (0.02 ml, 0.350 mmol) was added and the resulting mixture was stirred at room temperature for 15'. The crude solution was evaporated and purified with chromatography column in silica gel (*n*-Hexane/ AcOEt 85:15)

^{1}H NMR ($CDCl_3$) δ ppm:

2.54 (s, 3H); 4.16 (s, 2H); 7.20- 7.25 (m, 3H); 7.28-7.33 (m, 2H); 7.43-7.46 (m, 2H); 7.51-7.55 (m, 3H)

24

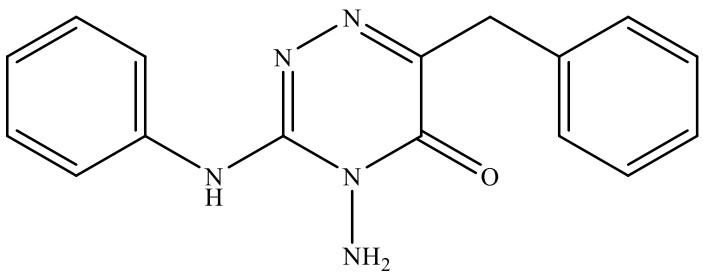

4-amino-6-benzyl-3-(phenylamino)-1,2,4-triazin-5(4*H*)-one

To a stirred solution of compound **17** (479.6 mg, 1.55 mmol) in isopropyl alcohol (5.46 ml) in a flame-dried two-necked round bottomed flask, hydrazine (1.09 ml) was added under argon atmosphere. The resulting mixture was refluxed at 105°C for 3h. After cooling at RT, the crude solution was dried, concentrated and purified with a silica gel column (*n*-Hexane / AcOEt 6:4) to afford compound **24** (200 mg, 0.682 mmol) as a white-yellow solid. The yield of this reaction was 44%.

^{1}H NMR ($CDCl_3$) δ ppm:

4.11 (s, 2H); 4.63 (bs, 1H); 7.12- 7.17 (m, 1H); 7.19- 7.24 (m, 1H); 7.28-7.31 (m, 2H); 7.34-7.39 (m, 2H); 7.40-7.43 (m, 2H); 7.65-7.69 (m, 2H)

1

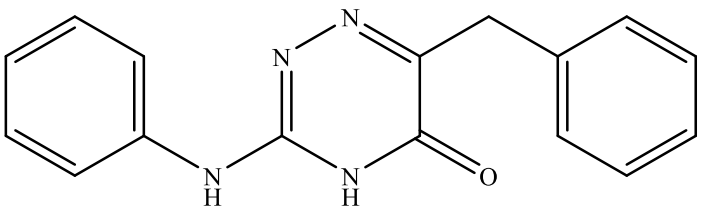

6-benzyl-3-(phenylamino)-1,2,4-triazin-5(4*H*)-one

Compound **24** (121.7 mg, 0.415 mmol) was dissolved, under inert atmosphere, in EtOH (6.08 ml). To resulting solution, concentrated hydrochloric acid (1.22 ml) was dropwise added in an ice bath. Finally, cold $NaNO_2$ 10% (3.04 ml) was added and the mixture was stirred, at room temperature, overnight. The reaction mixture was extracted with AcOEt and the organic phase was dried and evaporated. The crude product was purified with chromatography column in silica gel (CH_3Cl / CH_3OH 98:2) to afford a compound **1** (78 mg, 0.280 mmol) as a white, voluminous solid with a yield of 68%.

^{1}H NMR (DMSO-d_6) δ ppm:

3.81 (s, 2H); 7.08 (tt, 1H, *J*= 7.4, 2.0); 7.17-7.22 (m, 1H); 7.25-7.29 (m, 4H); 7.30-7.35 (m, 2H); 7.47-7.51 (m, 2H); 9.24 (bs, 1H); 12.07 (bs, 1H)

^{13}C NMR (DMSO-d_6) δ ppm:

35.92; 121.24 (2C); 123.55 ; 126.23 ; 128.22 (2C); 128.72 (2 C); 129.05 (2C); 137.55 ; 137.70 ; 148.80 ; 153.46 ; 162.35

37

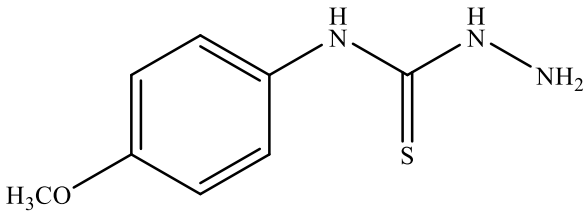

N-(4-methoxyphenyl)hydrazinecarbothioamide

A solution of NH_2NH_2 hydrate (0.16 ml, 5.09 mmol) in isopropyl alcohol (40 ml) was stirred in a flame-dried two-necked flask, under inert atmosphere. Then, 4-methoxyphenyl isothiocyanate (0.59 ml, 4.24 mmol) was added. Once the addiction was completed, stirring was continued for 1h at room temperature. The crude product was purified by a filtration with a glass septum. Finally, the white solid obtained (compound **37**, 747.4 mg, 3.79 mmol) was dried under reduced pressure. The yield of this reaction was 89%.

^{1}H NMR (DMSO-d_6) δ ppm:

3.73 (s, 3H); 4.70 (bs, 2H); 6.84-6.88 (m, 2H); 7.43-7.46 (m, 2H); 8.97 (bs, 1H); 9.49 (bs, 1H)

11

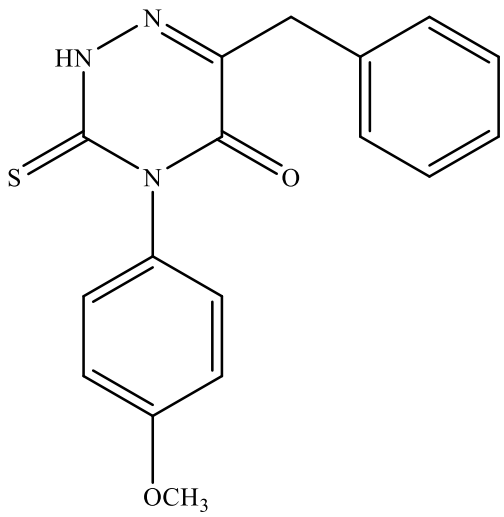

6-benzyl-4-(4-methoxyphenyl)-3-thioxo-3,4-dihydro-1,2,4-triazin-5(2*H*)-one

To the compound **8** (631.8 mg, 2.53 mmol) in a two-necked round bottomed flask, a solution of KOH 1M (7.59 ml, 7.59 mmol) was added. The mixture was refluxed at 115 °C for 4h. After cooling at room temperature, it was acidified, in an ice bath, with acetic acid. Then, compound **37** (500 mg, 2.53 mmol) in EtOH (7.59 ml) was added. The resulting solution was stirred and refluxed at 105 °C for 5 h. The reaction mixture was extracted with AcOEt . The organic phase was dried and evaporated under reduced pressure. The crude product was purified by a column chromatography in silica gel (*n*-Hexane / AcOEt 85:15) to afford compound **11** (223.9 mg, 0.683 mmol) as a yellow solid with a yield of 27%.

^{1}H NMR ($CDCl_3$) δ ppm:

3.84 (s, 3H); 3.97 (s, 2H); 7.01 (AA'XX', 2H, J_{AX}= 9, $J_{AA'/XX'}$= 2.7); 7.08-7.12 (m, 2H); 7.25-7.36 (m, 5H); 10.35 (bs, 1H)

18

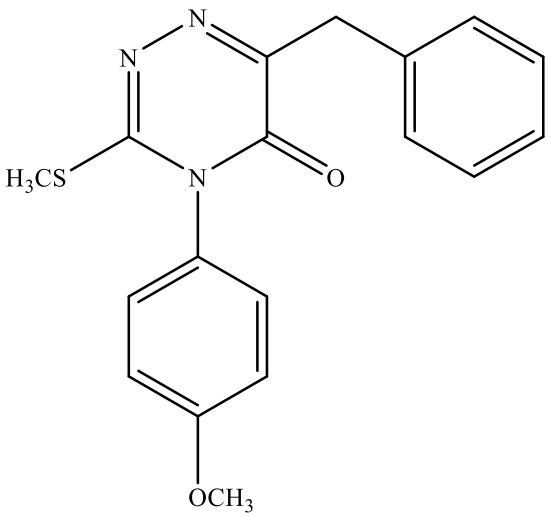

6-benzyl-4-(4-methoxyphenyl)-3-(methylthio)-1,2,4-triazin-5(4*H*)-one

A solution of compound **11** (223.9 mg, 0.688 mmol) in CH_3OH (0.69 ml) under argon was cooled and treated with a solution of CH_3ONa/CH_3OH (0.16 ml, 0.688 mmol). Then CH_3I (0.05 ml, 0.712 mmol) was added and the resulting mixture was stirred at room temperature for 15'. The crude solution was evaporated and was used in the next step without any further purification.

25

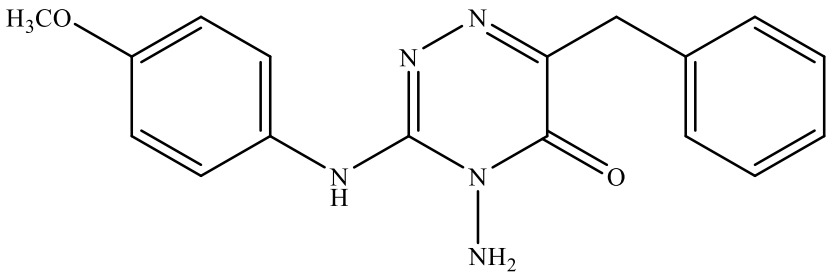

4-amino-6-benzyl-3-((4-methoxyphenyl)amino)-1,2,4-triazin-5(4*H*)-one

To a stirred solution of compound **18** (233.49 mg, 0.688 mmol) in isopropyl alcohol (5.00 ml) in a flame-dried two-necked round bottomed flask, hydrazine (0.48 ml) was added under argon atmosphere. The resulting mixture was refluxed at 105 °C for 3 h. After cooling at RT, the crude solution was dried, concentrated and purified with a silica gel column (*n*-Hexane / AcOEt 6:4) to afford compound **25** (60 mg, 0.186 mmol) as a white-yellow solid. The yield of this reaction was 27%.

^{1}H NMR ($CDCl_3$) δ ppm:

3.80 (s, 3H); 4.09 (s, 2H); 6.87-6.91 (m, 2H); 7.18- 7.23 (m, 1H); 7.27-7.32 (m, 2H); 7.39-7.42 (m, 2H); 7.51-7.56 (m, 2H)

2

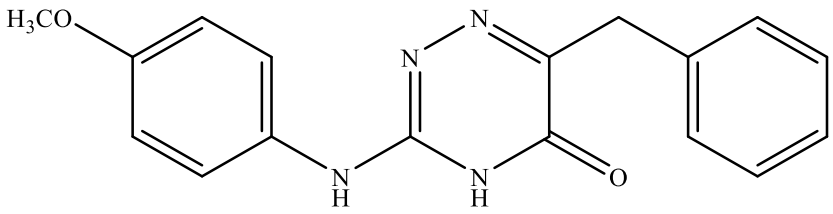

6-benzyl-3-((4-methoxyphenyl)amino)-1,2,4-triazin-5(4*H*)-one

Compound **25** (60.0 mg, 0.186 mmol) was dissolved, under inert atmosphere, in EtOH (3.00 ml). To resulting solution, concentrated hydrochloric acid (0.60 ml) was dropwise added in an ice bath. Finally, cold $NaNO_2$ 10% (1.50 ml) was added and the mixture was stirred, at room temperature, overnight. The reaction mixture was extracted with AcOEt and the organic phase was dried and evaporated. The crude product was purified with two chromatography columns in silica gel: the first (CH_3Cl / CH_3OH 98:2) and the second (*n*-Hexane / AcOEt 3:7) to afford a compound **2** (32.7 mg, 0.108 mmol) as a white-yellow solid with a yield of 58%.

^{1}H NMR (DMSO) δ ppm:

3.73 (s, 3H); 3.79 (s, 2H); 6.90 (AA'XX', 2H, J_{AX}= 9, $J_{AA'/XX'}$= 2.9); 7.17- 7.21 (m, 1H); 7.24- 7.30 (m, 4H); 7.34 (AA'XX', 2H, J_{AX}= 8.9, $J_{AA'/XX'}$= 2.7); 9.02 (bs, 1H); 11.98 (bs, 1H)

^{13}C NMR (DMSO-d_6) δ ppm:

35.88 ; 55.25 ; 113.77 ; 114.01 (2C); 120.52 ; 123.98 ; 126.20 ; 128.20 ; 129.04 (2C); 130.11 ; 137.65 ; 148.57 ; 153.82 ; 156.08 ; 162.46

9

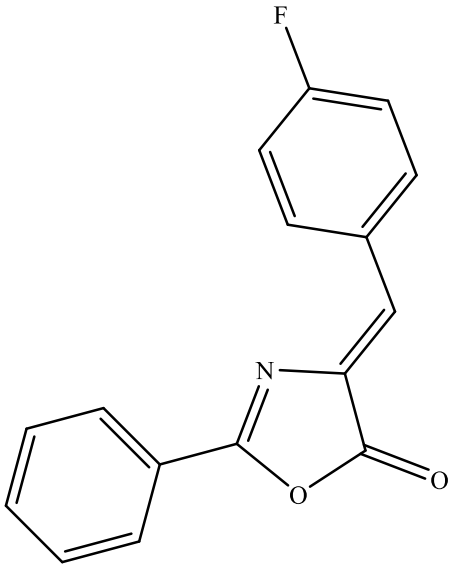

(*Z*)-4-(4-fluorobenzylidene)-2-phenyloxazol-5(4*H*)-one

Under argon atmosphere,4-fluorobenzaldehyde (1.11 ml, 10.32 mmol), acetic anhydride (2.92 ml, 30.96 mmol), hippuric acid (1850 mg, 10.32 mmol) and potassium acetate (1013 mg, 10.32 mmol) were inserted in a flame-dried double-necked round flask. The mixture was refluxed at 90 °C for 2h. After cooling at RT, the crude mixture was extracted with AcOEt. The organic phase was dried and concentrated. The crude product was purified by washing with distilled Hexane and was obtained the compound **9** (2.28 mg, 8.30 mmol) as a yellow, voluminous solid. The yield of this reaction was 80%.

^{1}H NMR ($CDCl_3$) δ ppm:

7.18 (double AA'XX', 2H, J_{AX}= 8.6, $J_{AA'/XX'}$= 2.5, $J_{HF\text{-}o}$= 9.6); 7.22 (s, 1H); 7.52-7.57 (m, 2H); 7.63 (tt, J= 7.4, 1.2); 8.17-8.21 (m, 2H); 8.25 (double AA'XX', 2H, J_{AX}= 9; $J_{AA'/XX'}$= 2.5, $J_{HF\text{-}m}$= 5.4)

12

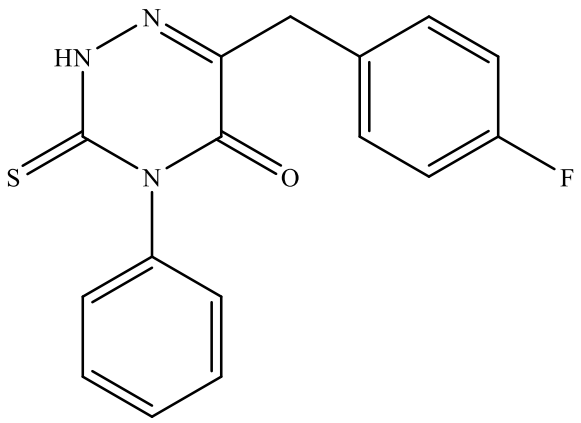

6-(4-fluorobenzyl)-4-phenyl-3-thioxo-3,4-dihydro-1,2,4-triazin-5(2*H*)-one

To the compound **9** (935 mg, 3.50 mmol) in a two-necked round bottomed flask, a solution of KOH 1M (10.49 ml, 10.49 mmol) was added. The mixture was refluxed at 115 °C for 4h. After cooling at room temperature, it was acidified, in an ice bath, with acetic acid. Then 4-phenyl thiosemicarbazide (585.3 mg, 3.50 mmol) in EtOH (10.49 ml) was added. The resulting solution was stirred and refluxed at 105°C for 5h. The reaction mixture was extracted with AcOEt . The organic phase was dried and evaporated under reduced pressure. The crude product was purified by a column chromatography in silica gel (*n*-Hexane / AcOEt 9:1) to afford compound **12** (610.3 mg, 1.95 mmol) as a glassy solid with a yield of 55%.

^{1}H NMR ($CDCl_3$) δ ppm:

3.94 (s,2H); 7.01 (double AA'XX', 2H, J_{AX}= 8.6, $J_{AA'/XX'}$= 2.5, $J_{HF\text{-}o}$= 9.5); 7.16-7.20 (m, 2H); 7.31 (double AA'XX', 2H, J_{AX}= 8.6, $J_{AA'/XX'}$= 2.6, $J_{HF\text{-}m}$= 5.4); 7.46-7.56 (m, 3H); 10.35 (bs, 1H)

19

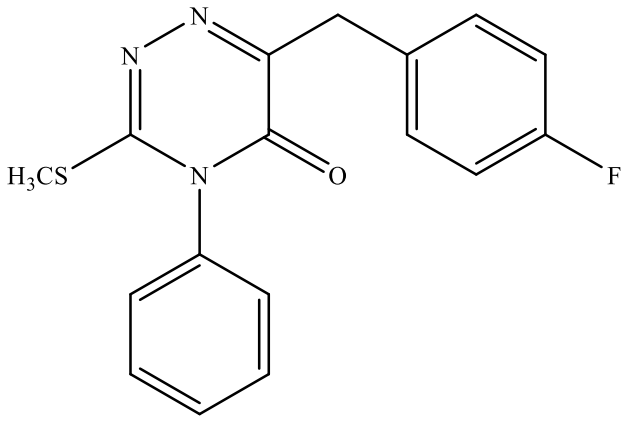

6-(4-fluorobenzyl)-3-(methylthio)-4-phenyl-1,2,4-triazin-5(4*H*)-one

A solution of compound **12** (280 mg, 0.894 mmol) in CH_3OH (0.89 ml) under argon was cooled and treated with a solution of CH_3ONa/CH_3OH (0.21 ml, 0.894 mmol). Then CH_3I (0.06 ml, 0.926 mmol) was added and the resulting mixture was stirred at room temperature for 15'. The crude solution was evaporated and was used in the next step without any further purification.

26

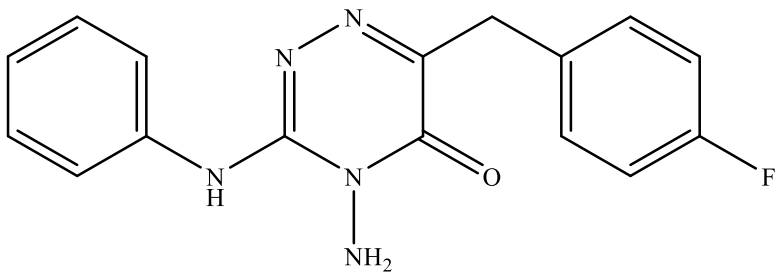

4-amino-6-(4-fluorobenzyl)-3-(phenylamino)-1,2,4-triazin-5(4*H*)-one

To a stirred solution of compound **19** (292.7 mg, 0.894 mmol) in isopropyl alcohol (3.15 ml) in a flame-dried two-necked round bottomed flask, hydrazine (0.63 ml) was added under argon atmosphere. The resulting mixture was refluxed at 105 °C for 3 h. After cooling at RT, the crude solution was dried, concentrated and purified with a silica gel column (*n*-Hexane / AcOEt 7:3) to afford compound **26** (79.7 mg, 0.256 mmol) as a white-yellow solid. The yield of this reaction was 29%.

^{1}H NMR ($CDCl_3$) δ ppm:

4.05 (s, 2H); 6.95- 6.99 (m, 2H); 7.16- 7.21 (m, 1H); 7.34-7.40 (m, 4H); 7.60-7.63 (m,2H)

3

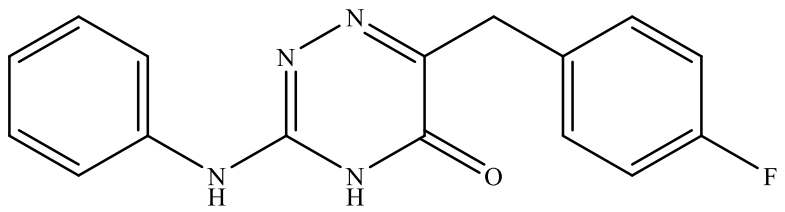

6-(4-fluorobenzyl)-3-(phenylamino)-1,2,4-triazin-5(4*H*)-one

Compound **26** (79.9 mg, 0.256 mmol) was dissolved, under inert atmosphere, in EtOH (3.98 ml). To resulting solution, concentrated hydrochloric acid (0.80 ml) was dropwise added in an ice bath. Finally, cold NaNO2 10% (1.99 ml) was added and the mixture was stirred, at room temperature, overnight. The reaction mixture was extracted with AcOEt and the organic phase was dried and evaporated. The crude product was purified by chromatography column in silica gel ($CHCl_3$ / CH_3OH 98:2) to afford compound **3** (23.8 mg, 0.080 mmol) as a white solid with a yield of 31%.

^{1}H NMR (DMSO-d_6) δ ppm:

3.80 (s, 2H); 7.06- 7.13 (m,3H); 7.28- 7.35 (m, 4H); 7.47- 7.50 (m, 2H); 9.23 (bs, 1H); 12.06 (bs, 1H)

^{13}C NMR (DMSO-d_6) δ ppm:

35.09 ; 114.86 (d, 2C, *J*= 21.1); 121.28 ; 123.58 ; 128.70 (3C); 130.73 (d, 2C, *J*= 8.0); 133.56 (d, 2C, *J*= 3.0); 137.61 ; 148.67 ; 153.41 ; 160.91 (d, 1C, *J*= 242.3)

13

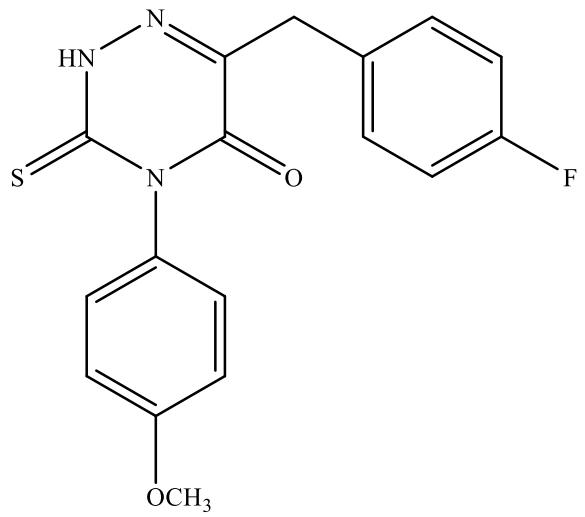

6-(4-fluorobenzyl)-4-(4-methoxyphenyl)-3-thioxo-3,4-dihydro-1,2,4-triazin-5(2*H*)-one

To the compound **9** (935 mg, 3.50 mmol) in a two-necked round bottomed flask, a solution of KOH 1M (10.49 ml, 10.49 mmol) was added. The mixture was refluxed at 115 °C for 4 h. After cooling at room temperature, it was acidified, in an ice bath, with acetic acid. Then compound **37** (690.48 mg, 3.50 mmol) in EtOH (10.49 ml) was added. The resulting solution was stirred and refluxed at 105 °C for 5 h. The reaction mixture was extracted with AcOEt . The organic phase was dried and evaporated under reduced pressure. The crude product was purified by a column chromatography in silica gel (*n*-Hexane / AcOEt 85:15) to afford compound **13** (548.6 mg, 1.60 mmol) as a white / yellow solid with a yield of 46%.

^{1}H NMR ($CDCl_3$) δ ppm:

3.84 (s, 3H); 3.94 (s, 2H); 6.98 - 7.03 (m, 4H); 7.09 - 7.12 (m, 2H); 7.29- 7.33 (m, 2H)

20

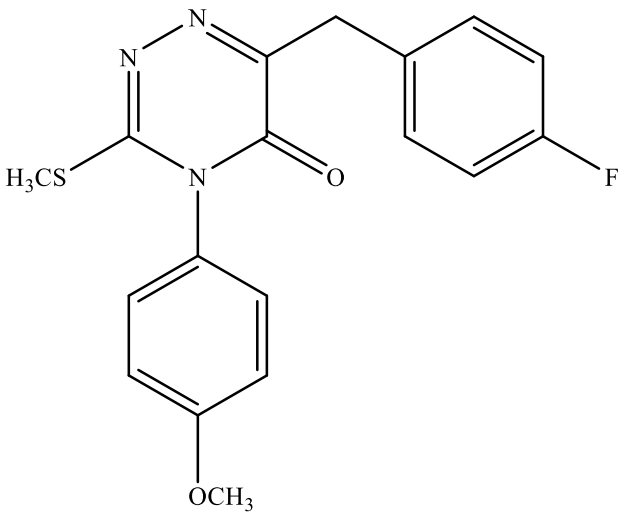

6-(4-fluorobenzyl)-4-(4-methoxyphenyl)-3-(methylthio)-1,2,4-triazin-5(4*H*)-one

A solution of compound **13** (350 mg, 1.02 mmol) in CH_3 OH (1.02 ml) under argon was cooled and treated with a solution of CH_3 ONa/CH_3 OH (0.24 ml, 1.02 mmol). After CH_3 I (0.07 ml, 1.06 mmol) was added and the resulting mixture was stirred at room temperature for 15'. The crude solution was evaporated and was used in the next step without any further purification.

27

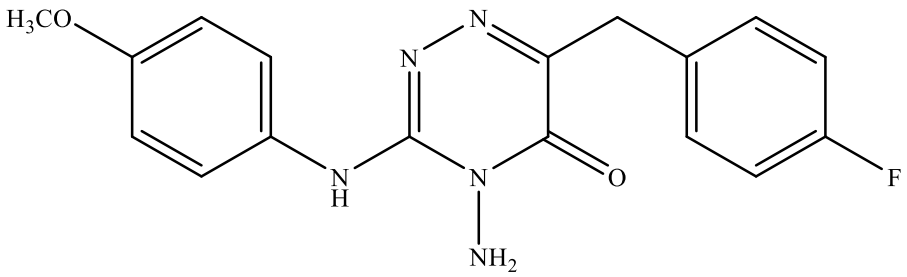

4-amino-6-(4-fluorobenzyl)-3-((4-methoxyphenyl)amino)-1,2,4-triazin-5(4*H*)-one

To a stirred solution of compound **20** (364.6 mg, 1.02 mmol) in isopropyl alcohol (3.59 ml) in a flame-dried two-necked round bottomed flask, hydrazine (0.72 ml) was added under argon atmosphere. The resulting mixture was refluxed at 105 °C for 3 h. After cooling at RT, the crude solution was dried, concentrated and purified with a silica gel column (*n*-Hexane / AcOEt 65:35) to afford compound **27** (112.6 mg, 0.330 mmol) as a white-yellow solid. The yield of this reaction was 32%.

^{1}H NMR ($CDCl_3$) δ ppm:

3.79 (s, 3H); 4.03 (s, 2H); 6.86- 6.90 (m, 2H); 6.94- 6.99 (m, 2H); 7.34 (double AA'XX', 2H, J_{AX}= 8.6, $J_{AA'/XX'}$= 2.0, $J_{HF\text{-}m}$= 5.4); 7.46- 7.49 (m, 2H)

4

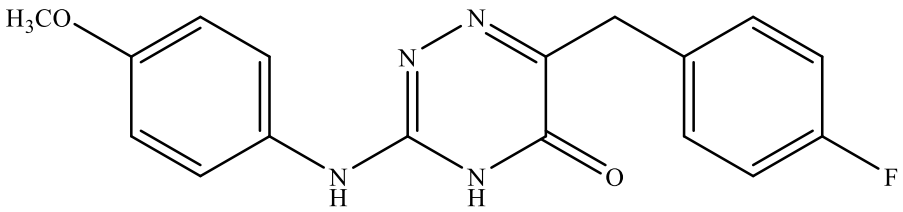

6-(4-fluorobenzyl)-3-((4-methoxyphenyl)amino)-1,2,4-triazin-5(4*H*)-one

Compound **27** (112.6 mg, 0.330 mmol) was dissolved, under inert atmosphere, in EtOH (5.63 ml). To resulting solution, concentrated hydrochloric acid (1.13 ml) was dropwise added in an ice bath. Finally cold $NaNO_2$ 10% (2.82 ml) was added and the mixture was stirred, at room temperature, overnight. The reaction mixture was extracted with AcOEt and the organic phase was dried and evaporated. The crude product was purified by chromatography column in silica gel (CH_2Cl_2 / CH_3OH 98:2; 95:5) to afford compound **4** (58.5 mg, 0.179 mmol) as a white solid with a yield of 54%.

^{1}H NMR (DMSO-d_6) δ ppm:

3.73 (s, 3H); 3.78 (s, 2H); 6.90 (AA'XX', 2H, J_{AX}= 9.1, $J_{AA'/XX'}$= 2.9); 7.1 (double AA'XX', 2H, J_{AX}= 9.0, $J_{AA'/XX'}$= 2.9, $J_{HF\text{-}o}$= 9.6); 7.29 (double AA'XX', 2H, J_{AX}= 8.8, $J_{AA'/XX'}$= 2.4, $J_{HF\text{-}m}$= 5.6); 7.33 (AA'XX', 2H, J_{AX}= 9.0, $J_{AA'/XX'}$= 2.8)

^{13}C NMR (DMSO-d_6) δ ppm:

35.08; 55.24; 114.01 (2C); 114.86 (d, 2C, J= 21.3); 124.01 (2C); 125.41; 130.06; 130.87 (d, 2C, J= 8.0); 133.68 (d, J= 3.0); 148.43; 153.80; 156.11; 160.92 (d, J= 240.5)

38

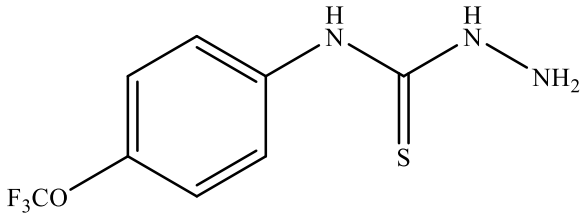

N-(4-(trifluoromethoxy)phenyl)hydrazinecarbothioamide

A solution of NH_2 NH_2 hydrate (0.08 ml, 2.74 mmol) in isopropyl alcohol (22.8 ml) was stirred in a flame-dried two-necked flask, under inert atmosphere. Then, 4-trifluoromethoxy phenyl isothiocyanate (0.37 ml, 2.28 mmol) was added. Once the addiction was completed, stirring was continued for 1h at room temperature. The crude product was purified by a filtration with a glass septum. Finally, the white solid obtained (compound **38**, 558.8 mg, 2.07 mmol) was dried under reduced pressure. The yield of this reaction was 91%.

^{1}H NMR (DMSO-d_6) δ ppm:

4.96 (bs, 2H); 7.28- 7.30 (m, 2H); 7.76- 7.78 (m, 2H); 9.24 (bs, 1H)

14

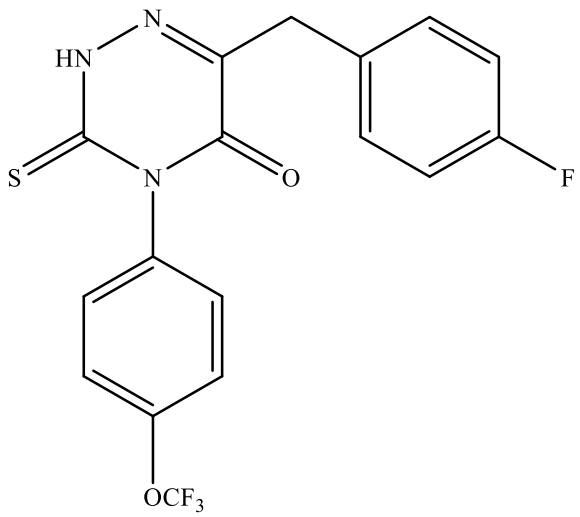

6-(4-fluorobenzyl)-3-thioxo-4-(4-(trifluoromethoxy)phenyl)-3,4-dihydro-1,2,4-triazin-5(2*H*)-one

To the compound **9** (552.6 mg, 2.06 mmol) in a two-necked round bottomed flask, a solution of KOH 1M (6.20 ml, 6.20 mmol) was added. The mixture was refluxed at 115°C for 4h. After cooling at room temperature, it was acidified, in an ice bath, with acetic acid. Then compound **38** (558.8 mg, 2.06 mmol) in EtOH (6.20 ml) was added. The resulting solution was stirred and refluxed at 105 °C for 5 h. The reaction mixture was extracted with AcOEt . The organic phase was dried and evaporated under reduced pressure. The crude product was purified by a column chromatography in silica gel (n-Hexane / AcOEt 85:15) to afford compound **14** (550.6 mg, 1.39 mmol) as an orange solid with a yield of 67%.

^{1}H NMR ($CDCl_3$) δ ppm:

3.94 (s, 2H); 6.99- 7.03 (m, 2H); 7.21- 7.26 (m, 2H); 7.30 (double AA'XX', 2H, J_{AX}= 8.8, $J_{AA'/XX'}$= 2.4, $J_{HF\text{-}m}$= 5.2); 10.45 (bs, 1H)

21

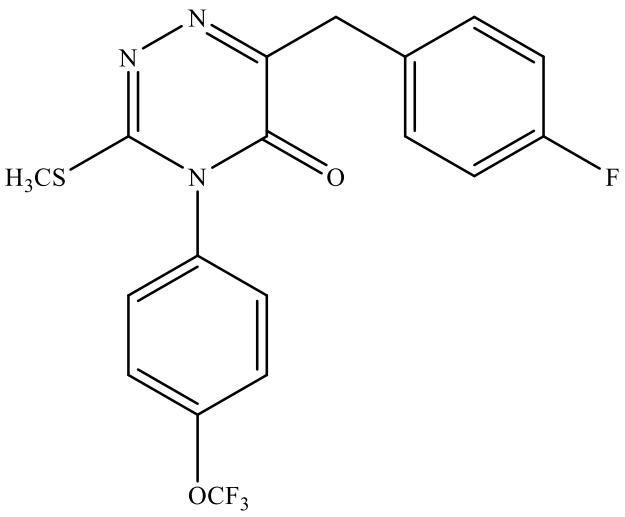

6-(4-fluorobenzyl)-3-(methylthio)-4-(4-(trifluoromethoxy)phenyl)-1,2,4-triazin-5(4*H*)-one

A solution of compound **14** (100 mg, 0.25 mmol) in CH_3 OH (0.25 ml) under argon was cooled and treated with a solution of CH_3ONa/CH_3OH (0.06 ml, 0.25 mmol). Then CH_3I (0.02 ml, 0.26 mmol) was added and the resulting mixture was stirred at room temperature for 15'. The crude solution was evaporated and was used in the next step without any further purification.

28

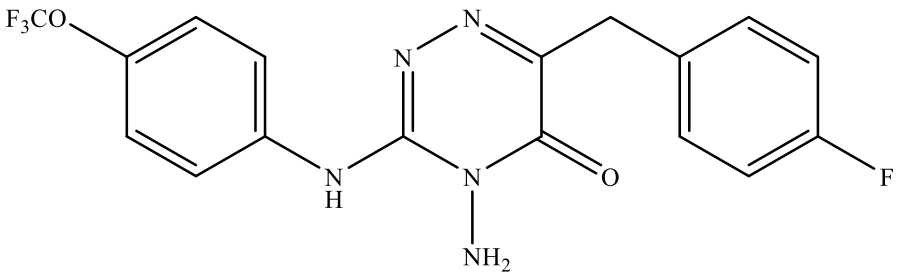

4-amino-6-(4-fluorobenzyl)-3-((4-(trifluoromethoxy)phenyl)amino)-1,2,4-triazin-5(4*H*)-one

To a stirred solution of compound **21** (464.88 mg, 1.13 mmol) in isopropyl alcohol (3.98 ml) in a flame-dried two-necked round bottomed flask, hydrazine (0.80 ml) was added under argon atmosphere. The resulting mixture was refluxed at 105 °C for 3 h. After cooling at RT, the crude solution was dried, concentrated and purified with a silica gel column (n-Hexane / AcOEt 8:2; 7:3) to afford compound **28** (132.4 mg, 0.335 mmol) as a yellow solid. The yield of this reaction was 30%.

^{1}H NMR ($CDCl_3$) δ ppm:

4.07 (s, 2H); 6.94- 6.98 (m, 2H); 7.20- 7.23 (m, 2H); 7.37 (double AA'XX', 2H, J_{AX}= 8.5, $J_{AA'/XX'}$= 2.4, $J_{HF\text{-}m}$= 5.4); 7.67- 7.71 (m, 2H)

5

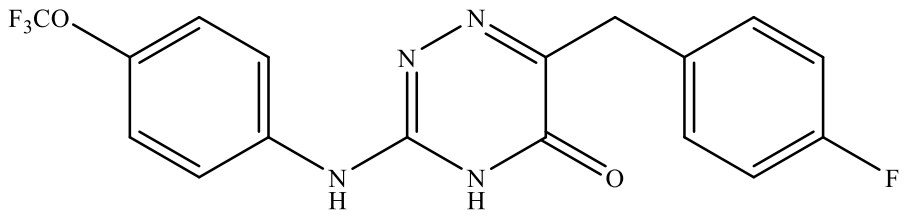

6-(4-fluorobenzyl)-3-((4-(trifluoromethoxy)phenyl)amino)-1,2,4-triazin-5(4*H*)-one

Compound **28** (132.4 mg, 0.335 mmol) was dissolved, under inert atmosphere, in EtOH (6.62 ml). To resulting solution, concentrated hydrochloric acid (1.32 ml) was dropwise added in an ice bath. Finally cold $NaNO_2$ 10% (3.31 ml) was added and the mixture was stirred, at room temperature, overnight. The reaction mixture was extracted with AcOEt and the organic phase was dried and evaporated. The crude product was purified by chromatography column in silica gel (CH_2 Cl_2 / CH_3 OH 98:2; 95:5) to afford compound **5** (30 mg, 0.079 mmol) as a white solid with a yield of 24%.

^{1}H NMR (DMSO-d_6) δ ppm:

3.80 (s, 2H); 7.10 (double AA'XX', 2H, J_{AX}= 8.9, $J_{AA'/XX'}$= 2.6, $J_{HF\text{-}o}$= 9.7); 7.28-7.34 (m, 4H); 7.60- 7.64 (m, 2H); 9.42 (bs,1H); 12.19 (bs, 1H)

^{13}C NMR (DMSO-d_6) δ ppm:

35.08; 114.86 (d, 2C, *J*= 21.1); 120.08 (q, *J*= 255.8); 121.50 (2C); 122.64 (2C); 130.89 (d, 2C, *J*= 8.0); 133.46 (d, *J*= 3.0); 136.96; 143.83; 148.98; 153.27; 160.92 (d, *J*= 242.0); 170.27

39

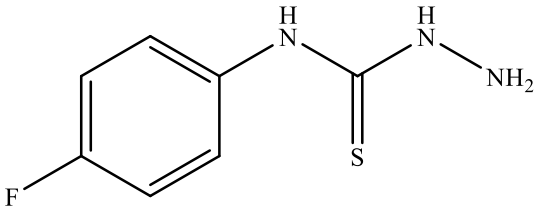

N-(4-fluorophenyl)hydrazinecarbothioamide

A solution of NH_2 NH_2 hydrate (0.12 ml, 3.91 mmol) in isopropyl alcohol (32.6 ml) was stirred in a flame-dried two-necked flask, under inert atmosphere. Then, 4-fluoro phenyl isothiocyanate (500 mg, 3.26 mmol) was added. Once the addiction was completed, stirring was continued for 1h at room temperature. The crude product was purified by a filtration with a glass septum. Finally, the white solid obtained (compound **39**, 474 mg, 2.56 mmol) was dried under reduced pressure. The yield of this reaction was 78%.

^{1}H NMR (DMSO-d_6) δ ppm:

4.78 (bs, 2H); 7.08 - 7.16 (m, 2H); 7.56 – 7.65 (m, 2H); 9.10 (bs, 1H)

15

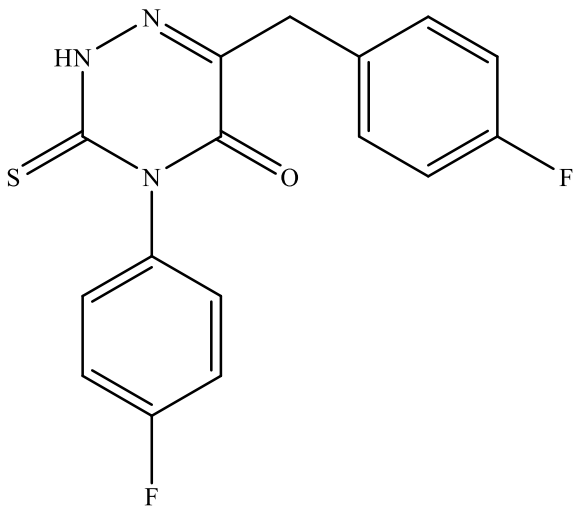

6-(4-fluorobenzyl)-4-(4-fluorophenyl)-3-thioxo-3,4-dihydro-1,2,4-triazin-5(2*H*)-one

To the compound **9** (686.8 mg, 2.56 mmol) in a two-necked round bottomed flask, a solution of KOH 1M (7.68 ml, 7.68 mmol) was added. The mixture was refluxed at 115 °C for 4 h. After cooling at room temperature, it was acidified, in an ice bath, with acetic acid. Then compound **39** (474 mg, 2.56 mmol) in EtOH (7.68 ml) was added. The resulting solution was stirred and refluxed at 105 °C for 5 h. The reaction mixture was extracted with AcOEt . The organic phase was dried and evaporated under reduced pressure. The crude product was purified by a column chromatography in silica gel (n-Hexane / AcOEt 85:15) to afford compound **15** (498.8 mg, 1.51 mmol) as an orange solid with a yield of 59%.

^{1}H NMR ($CDCl_3$) δ ppm:

3.94 (s, 2H); 7.01 (double AA'XX', 2H, J_{AX}= 8.8, $J_{AA'/XX'}$= 2.6, $J_{HF\text{-}o}$= 9.2); 7.15-7.23 (m, 4H); 7.29- 7.33 (m, 2H)

22

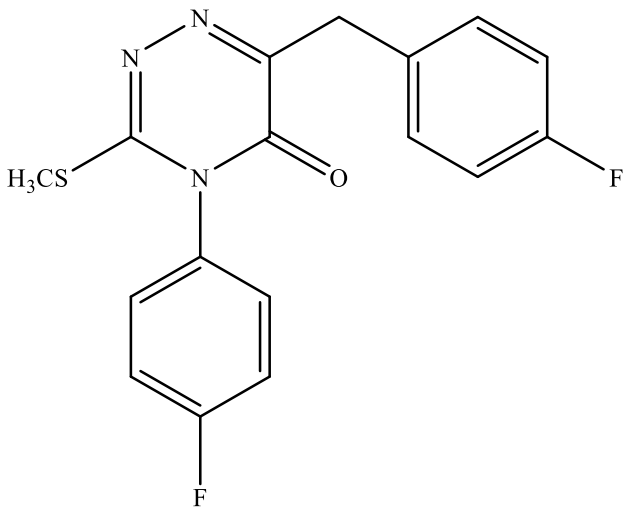

6-(4-fluorobenzyl)-4-(4-fluorophenyl)-3-(methylthio)-1,2,4-triazin-5(4*H*)-one

A solution of compound **15** (498.8 mg, 1.51 mmol) in CH_3 OH (1.51 ml) under argon was cooled and treated with a solution of CH_3 ONa/CH_3 OH (0.36 ml, 1.51 mmol). Then CH_3 I (0.12 ml, 1.56 mmol) was added and the resulting mixture was stirred at room temperature for 15'. The crude solution was evaporated and was used in the next step without any further purification.

29

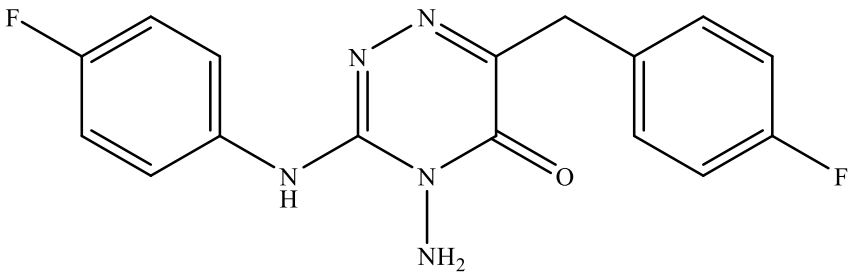

4-amino-6-(4-fluorobenzyl)-3-((4-fluorophenyl)amino)-1,2,4-triazin-5(4*H*)-one

To a stirred solution of compound **22** (521.5 mg, 1.51 mmol) in isopropyl alcohol (5.32 ml) in a flame-dried two-necked round bottomed flask, hydrazine (1.06 ml) was added under argon atmosphere. The resulting mixture was refluxed at 105 °C for 3 h. After cooling at RT, the crude solution was dried, concentrated and purified with a silica gel column (n-Hexane / AcOEt 8:2; 7:3; 6:4) to afford compound **29** (128.5 mg, 0.390 mmol) as a white solid. The yield of this reaction was 26%.

^{1}H NMR ($CDCl_3$) δ ppm:

4.06 (s, 2H); 4.66 (bs, 2H); 6.96 (double AA'XX', 2H, J_{AX}= 8.8, $J_{AA'/XX'}$= 2.6, $J_{HF\text{-}o}$= 9.7); 7.06 (double AA'XX', 2H, J_{AX}= 8.2, $J_{AA'/XX'}$= 2.7, $J_{HF\text{-}o}$= 8.7); 7.36 (double AA'XX', 2H, J_{AX}= 8.7, $J_{AA'/XX'}$= 2.6, $J_{HF\text{-}m}$= 5.5); 7.60 (double AA'XX', 2H, J_{AX}= 8.9, $J_{AA'/XX'}$= 2.9, $J_{HF\text{-}m}$= 4.7)

6

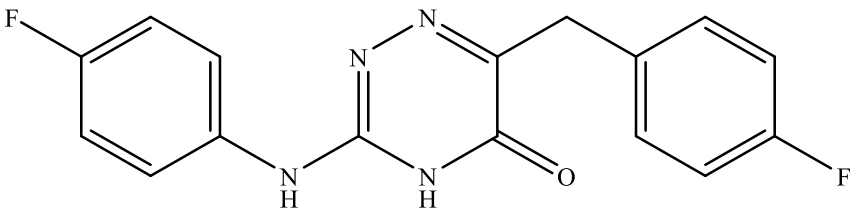

6-(4-fluorobenzyl)-3-((4-fluorophenyl)amino)-1,2,4-triazin-5(4*H*)-one

Compound **29** (128 mg, 0.390 mmol) was dissolved, under inert atmosphere, in EtOH (6.40 ml). To resulting solution, concentrated hydrochloric acid (1.28 ml) was dropwise added in an ice bath. Finally cold $NaNO_2$ 10% (3.20 ml) was added and the mixture was stirred, at room temperature, overnight. The reaction mixture was extracted with AcOEt and the organic phase was dried and evaporated. The crude product was purified by chromatography column in silica gel ($CHCl_3$ / CH_3OH 95:5; 95:5) to afford compound **6** (65.5 mg, 0.208 mmol) as a white solid with a yield of 53%.

^{1}H NMR (DMSO-d_6) δ ppm:

3.80 (s, 2H); 7.10 (double AA'XX', 2H, J_{AX}= 8.9, $J_{AA'/XX'}$= 2.6, $J_{HF\text{-}o}$= 9.6); 7.17 (double AA'XX', 2H, J_{AX}= 8.9, $J_{AA'/XX'}$= 2.9, $J_{HF\text{-}o}$= 10.4*);* 7.29 (double AA'XX', 2H, J_{AX}= 8.8, $J_{AA'/XX'}$= 2.6, $J_{HF\text{-}m}$= 5.6); 7.49 (double AA'XX', 2H, J_{AX}= 9.1, $J_{AA'/XX'}$= 2.9, $J_{HF\text{-}m}$= 4.9); 9.26 (bs, 1H); 12.11 (bs, 1H)

^{13}C NMR (DMSO-d_6) δ ppm:

35.05; 114.82 (d, 2C, *J*= 21.3); 115.27 (d, 2C, *J*= 22.1); 123.62 (d, 2C, *J*= 8.1); 130.84 (d, 2C, *J*= 8.1); 133.55 (d, *J*= 3.2); 133.82 (d, *J=2*.6); 148.68; 153.56; 157.31 ; 160.89 (d, *J*= 241.9); 161.00 (d, *J*= 256.2)

35

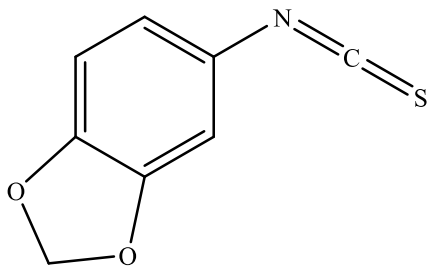

5-isothiocyanatobenzo[*d*][1,3]dioxole

Under argon atmosphere, CS_2 (0.66 ml, 10.92 mmol) and Et_3N (0.51 ml, 3.64 mmol) were added to a solution of 3, 4-(methylenedioxy)aniline (500 mg, 3.64 mmol) in EtOH (7.28 ml) at room temperature and the mixture was stirred for 30' in a flame-dried two-necked round bottomed flask. After being cooled using an ice bath, the reaction solution was treated with a solution of Boc_2O (794.2 mg, 10.92 mmol) in EtOH (3.64 ml) and DMAP. Once the addiction was completed, the stirring was continued for 5' in an ice bath and then for 20' at room temperature. The crude solution was evaporated and purified with a chromatography column in silica gel (*n*-Hexane / AcOEt 98:2) to afford compound **35** (480.9 mg, 2.68 mmol) as a white solid. The yield of reaction was 74%.

^{1}H NMR (DMSO-d_6) δ ppm:

6.10 (s, 2H); 6.96 (d, 2H, *J*= 1.2); 7.12 (t, 1H, *J*= 1.2)

40

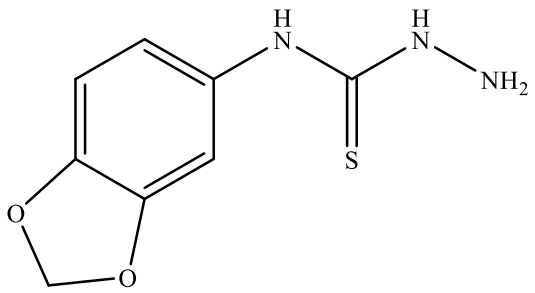

N-(benzo[*d*][1,3]dioxol-5-yl)hydrazinecarbothioamide

A solution of NH_2 NH_2 hydrate (0.08 ml, 2.74 mmol) in isopropyl alcohol (22.8 ml) was stirred in a flame-dried two-necked flask, under inert atmosphere. Then, compound **35** (480.9 mg, 2.68 mmol) was added. Once the addiction was completed, stirring was continued for 1h at room temperature. The crude product was purified by a filtration with a glass septum. Finally, the white solid obtained (compound **40**, 509.6 mg, 2.41 mmol) was dried under reduced pressure. The yield of this reaction was 90%.

^{1}H NMR (DMSO-d_6) δ ppm:

4.74 (bs, 2H); 6.00 (s, 2H); 6.83 (d, 1H, *J*= 8.0); 6.90 - 6.92 (m, 1H), 7.29 (bs, 1H); 9.04 (bs, 1H); 9.49 (bs, 1H)

16

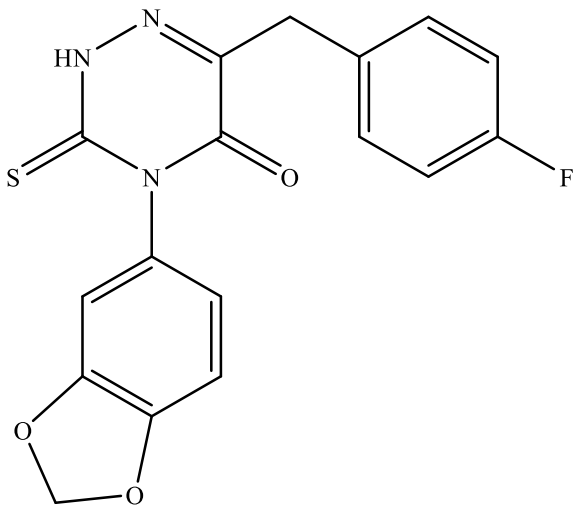

4-(benzo[*d*][1,3]dioxol-5-yl)-6-(4-fluorobenzyl)-3-thioxo-3,4-dihydro-1,2,4-triazin-5(2*H*)-one

To the compound **9** (456.1 mg, 1.70 mmol) in a two-necked round bottomed flask, a solution of KOH 1M (5.11 ml, 5.11 mmol) was added. The mixture was refluxed at 115 °C for 4 h. After cooling at room temperature, it was acidified, in an ice bath, with acetic acid. Then compound **40** (360 mg, 1.70 mmol) in EtOH (5.11 ml) was added. The resulting solution was stirred and refluxed at 105°C for 5h. The reaction mixture was extracted with AcOEt . The organic phase was dried and evaporated under reduced pressure. The crude product was purified by a column chromatography in silica gel (n-Hexane / AcOEt 85:15) to afford compound **16** (376.5 mg, 1.05 mmol) as a yellow solid with a yield of 62%.

^{1}H NMR ($CDCl_3$) δ ppm:

3.93 (s, 2H); 6.05 (d, 2H, *J*= 5.5); 6.63 - 6.66 (m, 2H); 6.91 (d, 1H, *J*= 7.6); 7.01 (double AA'XX', 2H, J_{AX}= 8.7, $J_{AA'/XX'}$= 2.5; $J_{HF\text{-}o}$= 9.5); 7.29- 7.33 (m, 2H)

23

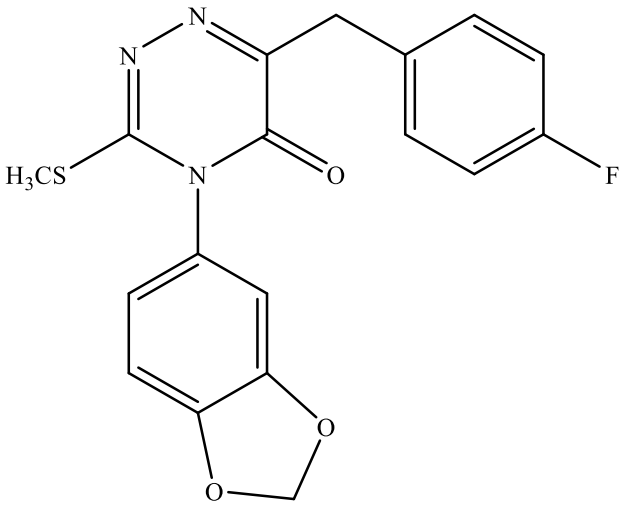

4-(benzo[*d*][1,3]dioxol-5-yl)-6-(4-fluorobenzyl)-3-(methylthio)-1,2,4-triazin-5(4*H*)-one

A solution of compound **16** (658.9 mg, 1.84 mmol) in CH_3 OH (1.84 ml) under argon was cooled and treated with a solution of CH_3ONa/CH_3OH (0.44 ml, 1.84 mmol). Then CH_3 I (0.12 ml. 1.90 mmol) was added and the resulting mixture was stirred at room temperature for 15'. The crude solution was evaporated and was used in the next step without any further purification.

30

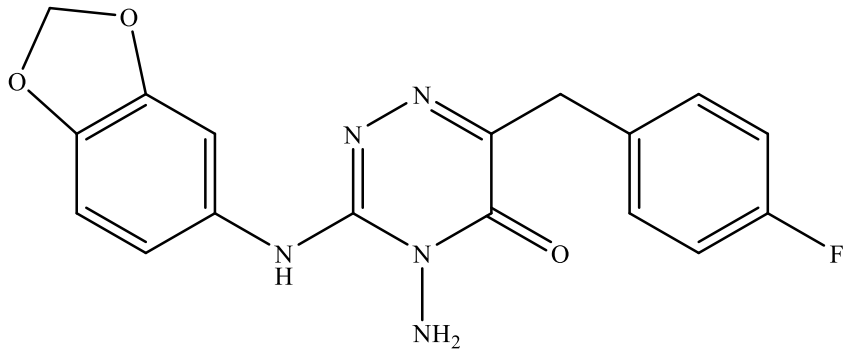

4-amino-3-(benzo[*d*][1,3]dioxol-5-ylamino)-6-(4-fluorobenzyl)-1,2,4-triazin-5(4*H*)-one

To a stirred solution of compound **23** (683.4 mg, 1.84 mmol) in isopropyl alcohol (6.48 ml) in a flame-dried two-necked round bottomed flask, hydrazine (1.30 ml) was added under argon atmosphere. The resulting mixture was refluxed at 105 °C for 3 h. After cooling at RT, the crude solution was dried, concentrated and purified with a silica gel column (n-Hexane / AcOEt 8:2) to afford compound **30** (151.2 mg, 0.43 mmol) as a white solid. The yield of this reaction was 23%.

^{1}H NMR ($CDCl_3$) δ ppm:

4.05 (s, 2H); 5.97 (s, 2H); 6.77 (d, 1H, J= 8.3); 6.91 (dd, 1H, J= 8.3, 2.2); 6.96 (double AA'XX', 2H, J_{AX}= 8.7, $J_{AA'/XX'}$= 2.5, $J_{HF\text{-}o}$= 9.5); 7.30 (d, 1H, J= 2.1); 7.35 (double AA'XX', 2H, J_{AX}= 8.7, $J_{AA'/XX'}$= 2.6, $J_{HF\text{-}m}$= 5.5)

7

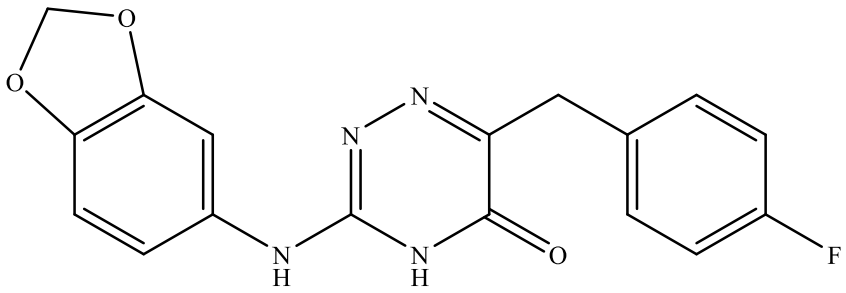

3-(benzo[*d*][1,3]dioxol-5-ylamino)-6-(4-fluorobenzyl)-1,2,4-triazin-5(4*H*)-one

Compound **30** (151.2 mg, 0.43 mmol) was dissolved, under inert atmosphere, in EtOH (7.56 ml). To resulting solution, concentrated hydrochloric acid (1.51 ml) was dropwise added in an ice bath. Finally cold $NaNO_2$ 10% (3.78 ml) was added and the mixture was stirred, at room temperature, overnight. The reaction mixture was extracted with AcOEt and the organic phase was dried and evaporated. The crude product was purified by chromatography column in silica gel (CH Cl_3 / CH_3 OH 95:5; 95:5) to afford compound **7** (11.2 mg, 0.33 mmol) as a yellow-white solid with a yield of 8%.

^{1}H NMR (DMSO-d_6) δ ppm:

3.79 (s, 2H); 6.01 (s, 2H); 6.80 (dd, 1H, *J*= 8.3, 2.1); 6.87 (d, 1H, *J*= 8.3); 7.07 - 7.14 (m, 3H); 7.29 (double AA'XX', 2H, J_{AX}= 8.7,$J_{AA'/XX'}$=2.4, $J_{HF\text{-}m}$= 5.6)

^{13}C NMR (DMSO-d_6) δ ppm:

35.11; 101.20; 104.73; 108.05; 114.91 (d, 2C, *J*= 21.2); 115.58; 130.94 (d, 2C, *J*= 8); 131.24; 133.63 (d, *J*= 3.4); 143.99; 147.22; 148.53; 153.78; 160.96 (d, *J*= 241.9); 162.46

6. Bibliography

[1] Elias, D.; Ditzel, H. J. Fyn is an important molecule in cancer pathogenesis and drug resistance. *Pharmacological Research 100* (**2015**) 250- 254.

[2] Kawakami, T.; Kawakami, Y.; Aaronson, S.A.; Robbins, K.C. Acquisition of transforming properties by FYN, a normal SRC-related human gene. *Proc. Natl. Acad. Sci. U.S.A.*, **1988**, *85*, 3870-3874.

[3] Yoshihito D. Saito, MD, MS; Ana R. Jensen, BS; Ravi Salgia, MD, phD; and Edwing M. Posadas, MD. Fyn, a novel molecular target in cancer. **2010**

[4] Brignatz, C.; Paronetto, M. P.; Opi, S.; Cappellari, M.; Audebert, S.; Feuillet, V.; Bismuth, G.; Roche, S.; Arold, S. T.; Sette, C.; and Collette, Y. Alternative splicing modulates autoinhibition in the Src kinase Fyn. *Molecular and Cellular Biology, Dec.***2009** *vol.*29, *No.*24, 6438- 6448.

[5] Goldsmith, J.F.; Hall, C.G.; Atkinson, T.P. Identification of an alternatively spliced isoform of the fyn tyrosine kinase. *Biochem. Biophys. Res. Commun.*, **2002**, *298*, 501-504.

[6] Kinoshita, T.; Matsubara, M.; Ishiguro, H.; Okita, K.; Tada, T. Structure of human Fyn kinase domain complexed with staurosporine. *Biochemical and Biophysical Research Communications, 346* (**2006**) 840- 844.

[7] Liang, X.; Lu, Y.; Wilkes, M.; Neubert, T. A.; and Resh, M. D. The N- terminal SH4 region of the Src family kinase Fyn is modified by methylation and heterogeneous fatty acylation. *The Journal of Biological Chemistry, Feb.* **2004** *vol.* 279, *No.* 9, 8133- 8139

[8] Salmond, R.J.; Filby, A.; Qureshi, I.; Caserta, S.; Zamoyska, R. T-cell receptor proximal signaling via the Src-family kinases, Lck and Fyn, influences T-cell activation, differentiation, and tolerance. *Immunol. Rev.*, **2009**, *228*, 9-22.

[9] Roskoski, R. Jr. Src protein- tyrosine kinase structure, mechanism, and small molecule inhibitors. *Pharmacological Research* 94 (**2015**) 9- 25.

[10] Boggon, T. J.; and Eck, M. J. Structure and regulation of Src family kinases. *Oncogene* (**2004**) *23* 7918- 7927.

[11] Hanks, S. K.; Quinn, A. M.; Hunter, T. The protein kinase family: conserved feature deduced phylogeny of the catalytic domains. *Science,* **1988**, 241, 42- 52.

[12] Lisbeth Schmidt Laursen, Colin W. Chan, and Charles ffrench- Constant. An integrin- contactin complex regulates CNS myelination by differential Fyn phosphorylation. *The Journal of Neuroscience, July 22*, **2009**, 29, 9174- 9185.

[13] Vacaresse, N.; Møller, B.; Danielsen, E. M.; Okada, M.; and Sap, J. Activation of c-Src and Fyn kinases by protein-tyrosine phosphatase RPTPα is substrate-specific and compatible with lipid raft localization. *The Journal of Biological chemistry*, *Vol.* 283, 35815- 35824, *Dec.***2008**.

[14] Chen, S.; Brier, S.; Smithgall, T. E.; and Engen, J. R. The Abl SH2-kinase linker naturally adopts a conformation competent for SH3 domain binding. *Dec.* **2006**.

[15] Gonfloni, S.; Williams, J. C.; Hattula, K.; Weijland, A.; Wierenga, R. K.; Superti-Furga, G. The role of the linker between the SH2 domain and catalytic domain in the regulation and function of Src. *The EMBO Journal* (**1997**), 16, 7261-7271.

[16] Okada, M. Regulation of the Src family kinases by Csk. *International Journal of Biological Science* **2012**, 1385- 1397.

[17] Nguyen, T-H; Liu, J.; Lombroso, P. J. Striatal enriched phosphatase 61 dephosphorylates Fyn at phosphotyrosine 420. *J Biol Chem*, 277, **2002**, 24274- 24279.

[18] Bhandari, V.; Lim, K. L.; and Pallen, C. J. Physical and functional interactions between receptor-like protein-tyrosine phosphatase α and $p59^{fin}$. *The Journal of Biological Chemistry. Vol* 273, *No*15 (**1998**), 8691- 8698.

[19] Sperber, B. R.; Boyle-Walsh, E. A.; Engleka, M. J.; Gadue, P.; Peterson, A. C.; Stein, P. L.; Scherer, S. S.; and McMorris, F. A. A unique role for Fyn in CNS Myelination. *The Journal of Neuroscience, March* **2001**, 2039- 2047.

[20] Klein, C.; Krämer, E. M.; Cardine, A. M.; Schraven, B.; Brandt, R.; and Trotter, J. Process outgrowth of oligodendrocytes is promoted by interaction of Fyn kinase with the cytoskeletal protein Tau. *The Journal of Neuroscience.* **2002**, 22, 698- 707.

[21] Belkadi, A.; and LoPresti, P. Truncated Tau with the Fyn-binding domain and without the microtubule-binding domain hinders the myelinating capacity of an oligodendrocyte cell line. *Journal of Neurochemistry* 2008, 107, 351- 360.

[22] Nada, S.; Shima, T.; Yanai, H.; Husi, H.; Grant, S.G.; Okada, M.; Akiyama, T. Identification of PSD-93 as a substrate for the Src family tyrosine kinase Fyn. *J. Biol. Chem*., **2003**, *278*, 47610-47621

[23] Sheng, M. The postsynaptic NMDA- receptor- PSD-95 signaling complex in excitatory synapses of the brain. *Journal of Cell Science*,**2001** 114, 1251.

[24] Trepanier, C. H.; Jackson, M. F.; and MacDonald, J. F. Regulation of NMDA receptors by the tyrosine kinase Fyn. *The Febs Journal*, 279, **2011**.

[25] Babus, L. W.; Little, E. M.; Keenoy, K. E.; Minami, S. S.; Chen, E.; Song, J. M.; Caviness, J.; Koo, S. Y.; Pak, D. T.; Rebeck, G.W.; Turner, R. S.; Hoe, H. S. Decreased dendritic spine density and abnormal spine morphology in Fyn knockout mice. *Brain Res* **2011**, 1415, 96- 102.

[26] Yang, K.; Belrose, J.; Trepanier, C. H.; Lei, G.; Jackson, M. F.; and MacDonald, J. F. Fyn, a potential target for Alzheimer's disease. *Journal of Alzheimer's disease,* 27, **2011**, 243- 252.

[27] Nygaard, H. B.; van Dyck, C. H.; and Strittmatter, S. M. Fyn kinase inhibition as a novel therapy for Alzheimer's disease. *Alzheimer's Research &* Therapy, **2014**, 6- 8.

[28] Lee, G.; Thangavel, R.; Vandana, M. S.; Joel, M. L.; Bhaskar, K.; Sandy, M. F.; Lana, H. D.; Andreadis, A.; Van Hoesen, G.; and Ksiezak- Reding, H. Phosphorylation of Tau by Fyn: implications for Alzheimer's disease. *The Journal of Neuroscience* (**2004**), 2304- 2312.

[29] Ittner, L. M. & Götz, J. Amyloid-β and Tau- a toxic *pas de deux* in Alzheimer's disease. *Nature Reviews Neuroscience*, 12, 67- 72, **2011**.

[30] Nakamura, T.; Yamashita, H.; Takahashi, T.; Nakamura, S. Activated Fyn phosphorylates alpha-synuclein at tyrosine residue 125.*Biochem Biophys Res Commun.* **2001**, 1085- 1092.

[31] Zhang, S.; Qi, Q.; Chan, C. B.; Zhou, W.; Chen, J.; Lou, H. R.; Appin, C.; Brat, D. J.; and Ye, K. Fyn- phosphorylated PIKE-A binds and inhibits AMPK signaling, blocking its tumor suppressive activity. *Cell Death Differ*. **2015**, 52-63.

[32] Tang, X.; Feng, Y.; and Ye, K. Src-family tyrosine kinase Fyn phosphorylates phosphatidylinositol 3-kinase enhancer- activating Akt, preventing its apoptotic cleavage and promoting cell survival. *Cell Death Differ*. **2007**, 368- 377.

[33] Chan, K. B.; and Ye, K. PIKE GTPase are phosphoinositide-3-kinse enhancers, suppressing programmed cell death. *J Cell Mol Med*.**2007**, 39- 53.

[34] Chen, R.; Kim, O.; Yang, J.; Sato, K.; Eisenmann, K. M.; McCarthy, J.; et al. Regulation of Akt/PKB activation by tyrosine phosphorylation. *J Biol Chem.* **2001**, 276, 31858- 31862.

[35] Baillat, G.; Siret, C.; Delamarre, E.; Luis, J. Early adhesion induces interaction of FAK and Fyn in lipid domains and activates raft- dependent Akt signaling in SW480colon cancer cells. *Molecular Cell Research. Vol.*1783, **2008**, 2323- 2331.

[36] Posadas, E. M.; Al-Ahmadie, H.; Robinson, V. L.; Jagadeeswaran, R.; Otto, K.;. Kasza, K. E.; Tretiakov, M.; Siddiqui, J.; Pienta, K. J.; Stadler, W. J.; Rinker-Schaeffer, C.; Salgia, R. Fyn is overexpressed in human prostate cancer. *Journal Compilation*, **2008**, 103, 171- 177.

[37] Liang, X.; Draghi, N. A.; and Resh, M. D. Signaling from integrins to Fyn to Rho family GTPases regulates morphologic differentiation of oligodendrocytes. *Journal of Neuroscience.* **2004**, 24, 7140- 7149.

[38] Mettouchi, A.; Klein, S.; Gou, W.; Lopez-Lago, M.; Lemichez, E.; Westwick, J.K.; and Giancotti, F. G. Integrin- specific activation of Rac controls progression through the G_1 phase of the cell cycle. *Molecular Cell. Vol*. 8. 115- 127, **2001**.

[39] Wary, K. K.; Mariotti, A.; Zurzolo, C.; and Giancotti, F. G. A requirement for Caveolin-1 and associated kinase Fyn in integrin signaling and anchorage- dependent cell growth. *Cell*. **1998**, 94, 625- 634.

[40] Kostic, A.; and Sheetz, M. P. Fibronectin rigidity response through Fyn and p130Cas recruitment to the leading edge. *Mol Biol Cell*. **2006**, 2684- 2695.

[41] Levin, B.; Sui, A.; Baker, C.; Dang, D.; Schinitt, R.; Eisapooran, P.; and Ramos, D. M. Expression of Fyn kinase modulates EMT in oral cancer cells. *Anticancer Research.***2010**, 30, 2591- 2596.

[42] Li, X.; Yang, Y.; Hu, Y.; Dang, D.; Regezi, J.; Schmidt, B. L.; Atakilit, A.; Chen, B.; Ellis, D.; and Ramos, D. M. αvβ6-Fyn Signaling Promotes Oral Cancer Progression. *The Journal of Biological Chemistry.Vol.*23, *No.*43, **2003**, 41646-41653.

[43] Hanke, J. H.; Gardner, J. P.; Dow, R. L.; Changelian, P. S.; Brissette, W. H.; Weringer, E. J.; Pollok, B. A.; and Patricia, A. Connely. Discovery of a novel, potent and Src family-selective tyrosine kinase inhibitor. *The Journal of Biological Chemistry. Vol*. 271, *No.*2, **1996**, 695- 701.

[44] Bishop, A.C.; Kung, C.; Shah, K.; Witucki, L.; Shokat, K.M.; Liu, Y. Generation of Monospecific Nanomolar Tyrosine Kinase Inhibitors via a Chemical Genetic Approach. *J. Am. Chem. Soc.* **1999**, 121, 627-631

[45] Summy, J.M.; Trevino, J.G.; Lesslie, D.P.; Baker, C.H.; Shakespeare, W.C.; Wang, Y.; Sundaramoorthi, R.; Metcalf, C.A.; Keats, J.A.; Sawyer, T.K.; Gallick, G.E. AP23846, a novel highly potent Src family kinase inhibitor, reduces vascular endothelial growth factor and interleukin-8 expression in human solid tumor cell lines and abrogates downstream angiogenic processes.

[46] Chen, P.; Doweyko, A. M.; Norris, D.; Gu, H. H.; Spergel, S. H.; Das, J.; Moquin, R. V.; Lin, J.; Wityak, J.; Iwanowicz, E. J.; McIntyre, K. W.; Shuster, D. J.; Behnia, K.; Chong, S.; de Fex, H.; Pang, S.; Pitt, S.; Shen, D. R.; Thrall, S.; Stanley, P.; Kocy, O. R.; Witmer, M. R.; Kanner, S. B.; Schieven, G. L.; and Barrish, J. C. Imidazoquinoxaline Src-Family Kinase p56Lck Inhibitors: SAR, QSAR, and the discovery of (S)-N-(2-Chloro-6-methylphenyl)-2-(3-methyl-1-piperazinyl)imidazo-[1,5-a]pyrido[3,2-e]pyrazin-6-amine (BMS-279700) as a potent and orally active inhibitor with excellent in vivo antiinflammatory activity. *J Med Chem.*47, **2004**, 4517- 4529.

[47] Rapecki, S.; and Allen, R. Inhibition of human T cell activation by novel Src kinase inhibitors is dependent upon the complexity of the signal delivered to the cell. *J. Pharmacol. Exp. Ther.*, **2002**, *303*, 1325-1333.

[48] Green, T.P.; Fennell, M.; Whittaker, R.; Curwen, J.; Jacobs, V.; Allen, J., Logie, A.; Hargreaves, J.; Hickinson, D.M.; Wilkinson, R.W.; Elvin, P.; Boyer, B.; Carragher, N.; Plé, P.A.; Bermingham, A.; Holdgate, G.A.; Ward, W.H.; Hennequin, L.F.; Davies, B.R.,Costello, G.F. Preclinical anticancer activity of the potent, oral Src inhibitor AZD0530. *Mol. Oncol.*, **2009** Feb 7. [Epub ahead of print].

[49] Das, J.; Chen, P.; Norris, D.; Padmanabha, R.; Lin, J.; Moquin, R. V.; Shen, Z.; Cook, L. S.; Doweyko, A. M.; Pitt, S.; Pang, S.; Shen, D. R.; Fang, Q.; de Fex, H. F.; McIntyre, K. W.; Shuster, D. J.; Gillooly, K. M.; Behnia, K.; Schieven, G. L.; Wityak, J.; and Barrish, J. C. 2-Aminothiazole as a novel kinase inhibitor template. structure-activity relationship studies toward the discovery of N-(2-Chloro-6-methylphenyl)-2-[[6-[4-(2-hydroxyethyl)-1-piperazinyl)]-2-methyl-4-

pyrimidinyl]amino)]-1,3-thiazole-5-carboxamide (Dasatinib, BMS-354825) as a potent pan-Src kinase inhibitor. *J Med Chem.* 49, **2006**, 6819- 6832.

[50] Chen, P.; Norris, D.; Das, J.; Spergel, S. H.; Wityak, J.; Leith, L.; Zhao, R.; Chen, B. C.; Pitt, S.; Pang, S.; Shen, D. R.; Zhang, R.; De Fex, H. F.; Doweyko, A. M.; McIntyre, K. W.; Shuster, D. J.; Behnia, K.; Schieven, G. L.; and Barrish, J. C. Discovery of novel 2-(aminoheteroaryl)-thiazole-5-carboxamides as potent and orally active Src-family kinase p56Lck inhibitors. *Bioorganic & Medicinal Chemistry Letters.* 14, **2004**, 6061- 6066.

[51] Poli, G.; Tuccinardi, T.; Rizzoli, F.; Caligiuri, I.; Botta, L.; Granchi, C.; Ortore, G.; Minutolo, F.; Schenone, S.; and Martinelli, A. Identification of new kinase inhibitors using a FLAP-based approach. *J. Chem. Inf. Model.* **2013**, 53, 2538- 2547.

[52] Brandvold, K. R.; Steffey, M. E.; Fox, C. C.; Soellner, M. B. Development of a highly selective c-Src kinase inhibitor. *ACS Chem. Biol.* **2012**, 7, 1393−1398.

[53] Mansour, A. K.; Eid, M. M.; Hassan, R. A.; Haemers, A.; Pattyn, S. R.; Vanden Berghe, D. A.; and Van Hoof, L. *J Heterocycles Chem.* 25, **1988**, 279- 283.

[54] Erlenmeyer-Plöchl Azlactone Synthesis. Comprehensive Organic Name Reactions and Reagents. 217, **2010**, 997–1000.

[55] Munch, H.; Hansen, J. S.; Pittelkow, M.; Christensen, J. B.; Boas, U. A new efficient synthesis of isothiocyanates from amine using di-*tert*-butyl dicarbonate. *Tetrahedron Letters.*49, **2008**, 3117- 3119.